Global Biogeochemical Cycles

RESEARCH ARTICLE
10.1029/2020GB006551

Dissolved Organic Nitrogen Cycling in the South China Sea From an Isotopic Perspective

Run Zhang[1], Xingchen T. Wang[2], Haojia Ren[3], Jie Huang[4], Min Chen[1], and Daniel M. Sigman[5]

[1]College of Ocean and Earth Sciences, Xiamen University, Xiamen, China, [2]Department of Earth and Environmental Sciences, Boston College, Chestnut Hill, MA, USA, [3]Department of Geosciences, National Taiwan University, Taipei, Taiwan, [4]Ministry of Education Key Laboratory for Earth System Modeling/Department of Earth System Science, Tsinghua University, Beijing, China, [5]Department of Geosciences, Princeton University, Princeton, NJ, USA

Key Points:
- We report the first data set of dissolved organic nitrogen (DON) $\delta^{15}N$ from the South China Sea (SCS)
- DON concentration and $\delta^{15}N$ correlate negatively ($r = 0.70$) in the upper 75 m, suggesting DON consumption with an isotope effect of ~4.9‰
- Comparison with other data sets suggests that DON $\delta^{15}N$ rises in oceanic regions of net DON consumption

Correspondence to:
R. Zhang,
zhangrun@xmu.edu.cn

Citation:
Zhang, R., Wang, X. T., Ren, H., Huang, J., Chen, M., & Sigman, D. M. (2020). Dissolved organic nitrogen cycling in the South China Sea from an isotopic perspective. *Global Biogeochemical Cycles*, *34*, e2020GB006551. https://doi.org/10.1029/2020GB006551

Received 16 JAN 2020
Accepted 2 NOV 2020
Accepted article online 12 NOV 2020

Abstract Dissolved organic nitrogen (DON) is the dominant form of fixed nitrogen in most low and middle latitude ocean surface waters. Here, we report measurements of DON isotopic composition ($\delta^{15}N$) from the west South China Sea (SCS), with the goal of providing new insight into DON cycling. The concentration of DON in the surface ocean is correlated ($r = 0.70$, $p < 0.0001$) with chlorophyll *a* concentration, indicating DON production in these surface waters. The concentration and $\delta^{15}N$ of DON fall in a relatively narrow range in the surface ocean (4.6 ± 0.1 μM and 4.3 ± 0.2‰ vs. air, respectively; ±*SD*), similar to other ocean regions. The mean DON $\delta^{15}N$ above 50 m (4.5 ± 0.3‰) is similar to the $\delta^{15}N$ of nitrate in the "shallow subsurface" (i.e., immediately below the euphotic zone; 4.6 ± 0.2‰) but is higher than the $\delta^{15}N$ of suspended particles in the surface ocean (~2.3‰). This set of isotopic relationships has been observed previously (e.g., in the oligotrophic North Atlantic and North Pacific) and can be explained by the cycling of N between particulate organic nitrogen (PON), DON, and ammonium, in which an isotope effect associated with DON degradation preferentially concentrates ^{15}N in DON. Consistent with this view, a negative correlation ($r = 0.70$) between the concentration and the $\delta^{15}N$ of DON is observed in the upper 75 m, suggesting an isotope effect of ~4.9 ± 0.4‰ for DON degradation. Comparing the DON $\delta^{15}N$ data from the SCS with other regions, we find that the $\delta^{15}N$ difference between euphotic zone DON and shallow subsurface nitrate $\delta^{15}N$ ($\Delta\delta^{15}N_{(DON\text{-}NO3)}$) rises from ocean regions of inferred net DON production to regions of net DON consumption, with the SCS representing an intermediate case.

Plain Language Summary In most areas of the (sub)tropical surface ocean, dissolved inorganic nitrogen (e.g., nitrate) is fully consumed by phytoplankton as a critical nutrient in their growth. In contrast, the concentration of dissolved organic nitrogen (DON) in these waters is 1–3 orders of magnitude higher than dissolved inorganic nitrogen. The high concentration of DON in oligotrophic oceans is often explained as a result of its chemical recalcitrance, which prevents it from being rapidly assimilated and used by plankton. However, the concentration of DON does vary, and it may play an important role in upper ocean N cycle. In this study, DON in the South China Sea (SCS) was investigated for its concentration and natural isotopic composition (i.e., its ratio of heavier ^{15}N relative to lighter ^{14}N). We find evidence for both production and consumption of DON in the shallow waters of the SCS. Our findings thus support the possibility that DON is an important part of the upper ocean N cycle. In addition, a comparison of the SCS DON data with those from other ocean regions is consistent with previous suggestions of lateral transfer of DON from regions of upwelling and vertical mixing to lower-nutrient, more stratified tropical and subtropical waters.

1. Introduction

Dissolved organic nitrogen (DON) is the dominant form of biologically available nitrogen (fixed N) in most tropical and subtropical surface oceans, but its bioavailability and cycling remain enigmatic (Hansell et al., 2009; Knapp et al., 2005; Letscher et al., 2013; Sipler & Bronk, 2014). Although DON has traditionally been considered to have low lability, it has been argued that classifying all DON as refractory possibly overlooks an important source of available N in the marine environment (Bronk et al., 2007). Indeed, DON does contain compounds and functionalities that are believed to be readily bioavailable (Sipler & Bronk, 2014). Given the relatively high concentration of DON in the surface ocean, even modest reactivity could make

it an important proximal source of fixed N for biological productivity. Indeed, some studies have suggested that DON participates in and affects upper ocean biogeochemical cycling (Bronk et al., 2007; Knapp et al., 2018; Torres-Valdés et al., 2009). Further, extensive data sets of DON concentration and model simulations suggest that the subtropical gyre regions import DON from gyre margins (Letscher et al., 2016). Also, DON in the gyres may be mixed downward or subducted into the ocean interior prior to breakdown, thus representing a component of the biological pump in addition to sinking organic matter (Letscher et al., 2013).

Along with its concentration, the N isotopic composition of DON can be used to study DON cycling in the ocean (Benner et al., 1997; Feuerstein et al., 1997; Knapp et al., 2005, 2011). Prior work on DON $\delta^{15}N$ has mostly focused on the subtropical gyres of the North Atlantic and the North Pacific (Knapp et al., 2005, 2011; Yamaguchi & McCarthy, 2018). Recently, DON $\delta^{15}N$ has been reported in an oceanographic setting outside of the oligotrophic subtropical gyres, that is, the Eastern Tropical South Pacific (ETSP), providing new insights into the production and consumption of DON (Knapp et al., 2018).

The semienclosed South China Sea (SCS) is the largest tropical/subtropical marginal sea in the western Pacific. It is generally characterized by a shallow mixed layer and oligotrophic conditions, but it undergoes upwelling and vertical mixing on a seasonal basis, especially along its margins (Liu et al., 2010). The SCS is strongly influenced by the Asian monsoon, with southwesterly winds prevailing in summer (June–September) and northeasterly in winter (November–March). The basin-scale surface circulation responds to the winds, which drive an anticyclonic gyre in summer and a cyclonic gyre in winter (Hu et al., 2000). The upwelling and associated vertical mixing result in a relatively shallow nutricline, rapid nutrient supply, and thus somewhat elevated primary production relative to other tropical and subtropical open ocean regions (Gregg et al., 2003). Despite the relatively rapid supply of nutrients, N has been suggested to be a key limiting nutrient for primary production in the SCS (Chen et al., 2004). The nutrient supply into surface layers is characterized by excess phosphorus (N:P < 16), which has been suggested to encourage N_2 fixation in the SCS (Ren, Sigman, et al., 2017; Wong et al., 2007; Wu et al., 2003).

Prior studies had examined the isotopic composition of particulate N (PN) and nitrate in the SCS water column (Yang et al., 2017, 2018). There are few DON concentration measurements from the SCS (Hung et al., 2007; Xu et al., 2018), and there are not as yet any reported DON $\delta^{15}N$ measurements. DON concentrations in the mixed layer are 2–3 orders of magnitude higher than those of dissolved inorganic N (DIN) in the northern SCS basin (Hung et al., 2007). The potential importance of DON in upper water column N cycling calls for further study of this numerically dominant N pool.

In this study, we report the concentrations and $\delta^{15}N$ values of DON, suspended PN (PN_{susp}), and nitrate from the upper water column of western SCS (WSCS) (Figure 1). With this new data set, we seek to (1) obtain the spatial distribution of [DON] and the $\delta^{15}N$ of DON ($\delta^{15}N_{DON}$) in the WSCS, (2) examine the N isotope dynamics associated with DON production and consumption, and (3) compare the SCS data with measurements from other ocean regions.

2. Materials and Methods

2.1. Study Area

The samples were collected at deep basin stations (with depths of >2,000 m) in the WSCS (Figure 1). In summer, the sampling region is dominated by the Southeast Vietnam Offshore Current, a strong eastward jet (Hu et al., 2000). This eastward jet leaves the Vietnam coast between 10°N and 12°N and bifurcates in the vicinity of 113°E (Chen et al., 2010).

2.2. Field Sampling

Field sampling was conducted on Cruise NORC2015-07 of the R/V *Shiyan 3* during 17–27 September 2015 in the tropical WSCS (Figure 1), sampling the summer monsoon period. At 44 stations, seawater samples were collected for concentration of nitrate + nitrite analysis from seven depths (5, 25, 50, 75, 100, 150, and 200 m) with a Seabird SBE 911plus conductivity-temperature-density and rosette system. Out of the 44 stations, 25 were selected for DON and nitrate $\delta^{15}N$ analyses (Figure 1).

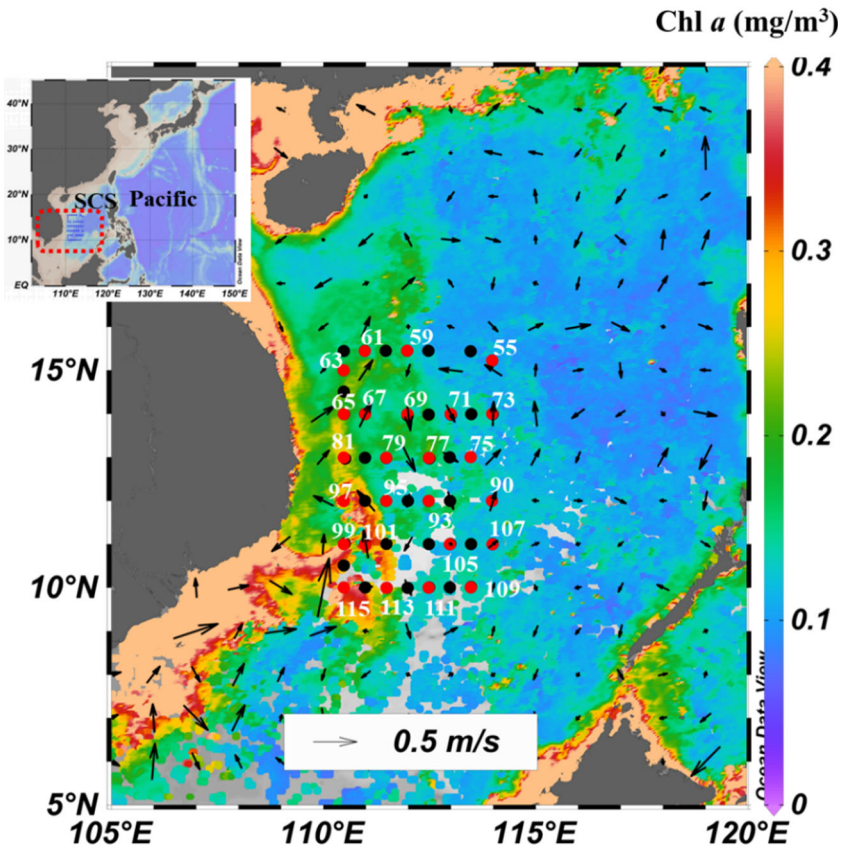

Figure 1. Sampling locations in the western SCS in September 2015. Water samples were collected from 44 stations (circles, station number indicated in white) at seven depths (5, 25, 50, 75, 100, 150, and 200 m). Nitrate concentrations were measured at all stations. A subset of stations (red circles, $n = 25$) were selected for measurement of $\delta^{15}N$ of DON and nitrate. Color map and arrows indicate mean sea surface Moderate Resolution Imaging Spectroradiometer chlorophyll *a* concentration and Archiving, Validation, and Interpretation of Satellite Oceanography geostrophic current during the period of the cruise, respectively.

2.2.1. Concentrations of Nitrate and Nitrite

Seawater samples for nitrate + nitrite (referred to as nitrate in section 3 and thereafter) or total dissolved nitrogen (TDN) were filtered through Millipore polycarbonate filters (0.2 μm). The filtrates were collected into acid-cleaned and sample-rinsed high-density polyethylene bottles (Nalgene), frozen, and stored at −20°C. The concentration of seawater nitrate + nitrite (referred to as $[NO_3^-]$ in section 3 and thereafter) was determined by the chemiluminescence method (Braman & Hendrix, 1989). Briefly, nitrate + nitrite was reduced to nitric oxide by an acidic solution of vanadium (V^{3+}) at 95°C. The nitric oxide was then quantified with a Teledyne 200 EU chemiluminescence analyzer. The detection limit was 0.01 μM, and the average precision based on replicate measurements was 3%.

2.2.2. Isotopic Composition of Nitrate and Nitrite

Nitrogen isotope ratios of seawater nitrate + nitrite was determined using the "denitrifier" method (Sigman et al., 2001) for samples with $[NO_3^-] > 0.3$ μM. Briefly, nitrate samples were reduced to nitrous oxide (N_2O) by the denitrifying bacterial strain *Pseudomonas chlororaphis ssp. aureofaciens* (ATCC 13985, Manassas, VA, USA) that lacks nitrous oxide reductase activity. The N isotopic composition of the N_2O product was measured at Princeton University on a Thermo MAT253 isotope ratio mass spectrometer coupled with a custom N_2O extraction system (Weigand et al., 2016). Two international reference materials were used for calibration (−1.8‰ for USGS34 and 4.7‰ for IAEA-NO-3, vs. air). The N isotope composition is expressed as

$$\delta^{15}N = \left(\frac{R_{Sample}}{R_{Standard}} - 1\right) \times 1000,$$

where R_{Sample} and $R_{Standard}$ represent the $^{15}N/^{14}N$ ratios of sample and air N_2, respectively. The average standard deviation of the $\delta^{15}N$ measurements on sample replicates was <0.1‰.

2.2.3. DON

Samples for DON measurements were collected from the same stations at four water depths (5, 25, 50, and 75 m). The concentration and $\delta^{15}N$ of TDN were measured by persulfate oxidation coupled to the denitrifier method following (Knapp et al., 2005), with minor modifications based on the fossil-bound organic matter $\delta^{15}N$ protocol (Ren et al., 2009; Wang et al., 2015). Briefly, in a precombusted 4 ml glass vial, 2 ml persulfate oxidizing reagent (POR) (1 g $K_2S_2O_8$ + 1.5 g NaOH in 100 ml purified low-N water) was added to 2 ml seawater sample, followed by autoclaving for 55 min. The pH of the resulting samples was then adjusted to near neutral. The resulting nitrate was analyzed for $\delta^{15}N$ using the denitrifier method described above. DON concentration was calculated by subtracting the concentrations of nitrate in the original samples from that of the oxidized samples ($[DON] = [TDN] - [NO_3^-]$). The isotopic composition of DON was calculated from isotopic mass balance. In each batch of samples, amino acid standards with known $\delta^{15}N$ (USGS40 and USGS41) as well as the blanks associated with persulfate reagent were measured and used in the blank correction following (Wang et al., 2018). The main source of nitrogen blank in the full protocol is associated with the oxidation step, and it comes largely from the POR. The concentrations of the measured POR blanks were less than 0.3 μM, composing no more than 6% of total N in oxidized samples. The average standard deviation for duplicate [DON] analyses was ±0.12 μM for samples with undetectable nitrate, and the propagated error for [DON] in the presence of detectable nitrate was ±0.14 μM. These two values are quite close, as the propagated error for [DON] is simple:

$$\sigma_{[DON]} = \sqrt{\sigma^2_{[TDN]} + \sigma^2_{[N03]}}.$$

For samples that contain detectable nitrate, an additional step was taken to calculate DON $\delta^{15}N$ based on mass balance (with measured nitrate concentration and $\delta^{15}N$):

$$\delta^{15}N_{DON} = \frac{\delta^{15}N_{TDN} \times [TDN] - \delta^{15}N_{NO3} \times [NO_3^-]}{[DON]}.$$

The uncertainties in [DON] and $\delta^{15}N$ were calculated from error propagation using the following equation (Ku, 1966):

$$\sigma_{\delta_{DON}} = \sqrt{\left(\frac{\partial\delta_{DON}}{\partial[TDN]}\right)^2 \times \sigma^2_{TDN} + \left(\frac{\partial\delta_{DON}}{\partial[NO_3]}\right)^2 \times \sigma^2_{[N03]} + \left(\frac{\partial\delta_{DON}}{\partial\delta_{TDN}}\right)^2 \times \sigma^2_{\delta_{TDN}} + \left(\frac{\partial\delta_{DON}}{\partial\delta_{NO3}}\right)^2 \times \sigma^2_{\delta_{NO3}}}.$$

The POR $\delta^{15}N$ correction for TDN analysis is generally between ~0‰ and ~0.2‰, with USGS40 and USGS41 as internal standards. The average standard deviation of $\delta^{15}N_{DON}$ for replicate samples with undetectable nitrate was 0.2‰. The propagated uncertainty of $\delta^{15}N_{DON}$ for samples that had $[NO_3^-]$ similar to [DON] was ±0.4‰.

2.2.4. Suspended PN

Suspended particles were collected in surface waters (from a depth of ~5 m, $n = 41$) by filtering ~20 L seawater onto precombusted (450°C, 4 hr) Advantec GF75 glass fiber (0.3 μm poresize) filters. Sample filters were stored frozen (−20°C) until analysis. The N content and isotopic composition of these filters were analyzed at Xiamen University on a Finnigan Delta V Advantage isotope ratio mass spectrometer interfaced with a Carlo Erba NC 2500 elemental analyzer. The standard deviation for these $\delta^{15}N$ measurements was ±0.2‰. Data set of N concentration and $\delta^{15}N$ for this study are available in Mendeley Data (https://data.mendeley.com/datasets/7k53k4nzc7/draft?a=b91ee88f-5355-4d64-ae04-080ac2955265).

2.2.5. Surface Chlorophyll *a*

Seawater-collected chlorophyll *a* data for each station are not available for this cruise. Instead, surface chlorophyll *a* concentration with 8 day temporal resolution and 9 km spatial resolution was taken from the

Moderate Resolution Imaging Spectroradiometer (MODIS; https://oceandata.sci.gsfc.nasa.gov/MODIS-Aqua), with averaging of the satellite data closest to each sampling location. In general, the MODIS product overestimates chlorophyll *a*, and its annual mean bias in the global ocean is ~8% (Gregg & Casey, 2007). The uncertainty in MODIS chlorophyll *a* for much of open ocean is less than ±35% (Moore et al., 2009). In the SCS, the MODIS product has been used extensively (e.g., Shang et al., 2011; Wang & Tang, 2014) and has been shown to be accurate (Liu et al., 2013; Zhang et al., 2006).

3. Results

3.1. Ancillary Environmental Measurements

Sea surface temperature ranged from 28.76°C to 30.31°C and averaged 29.66 ± 0.35°C (±*SD*), and sea surface salinity ranged from 32.48 to 33.73 practical salinity unit and averaged 33.20 ± 0.31. The lowest sea surface salinity were observed at the southwestern stations, consistent with freshwater input from the Mekong River plume (Voss et al., 2006). The distribution of surface chlorophyll *a* was patchy, with elevated phytoplankton biomass (chlorophyll *a* ~ 0.4 mg/m^3) as a narrow northeastward jet-shaped protrusion into the WSCS in the southern area during our sampling period (Figure 1). For the offshore stations further to the east, surface chlorophyll *a* decreased to ~0.1 mg/m^3, typical of tropical oligotrophic waters.

3.2. Nitrate Concentration and $\delta^{15}N$

Nitrate concentration ([NO_3^-]) was <20 nM in surface water (5 m) at all stations. In the upper 50 m, [NO_3^-] was generally <100 nM, except for northwestern station Sta. 61, where elevated nitrate concentration (1.8 μM) was observed at 25 m and deeper. The "nitracline" (defined as the depth at which [NO_3^-] equals 0.1 μM; Chen et al., 2008) was generally between 50 and 75 m (Figures 2 and 3a). Below the nitracline depth, [NO_3^-] increased progressively with depth. At 75 m, [NO_3^-] was 5.4 ± 4.2 μM, and N isotopic composition of nitrate (referred to as $\delta^{15}N_{NO3}$ hereafter) was 5.2 ± 0.8‰. Notably, a shallow subsurface minimum in $\delta^{15}N_{NO3}$ was observed at ~100 m at most stations, with a mean value of 4.6 ± 0.2‰ ([NO_3^-] = 10.5 ± 2.5 μM) (Figures 3a and 3d). Below the depth of the $\delta^{15}N_{NO3}$ minimum, both [NO_3^-] and $\delta^{15}N_{NO3}$ increased steadily with increasing depth, reaching 14.3 ± 3.2 μM and 5.3 ± 0.5‰ at 150 m and 18.0 ± 1.9 μM and 5.4 ± 0.2‰ at 200 m.

3.3. TDN Concentration and $\delta^{15}N$

The vertical pattern of [TDN] was mainly caused by [NO_3^-] because of the large gradient in its concentrations. [TDN] showed a similar vertical pattern as [NO_3^-], increasing with depth below ~50 m (Figures 3a and 3b). In the upper 50 m, TDN was predominantly composed of DON. The $\delta^{15}N$ of TDN showed little variation over the upper mixed layer (29 ± 7 m), with an increasing trend from 25 to 75 m, often with a sharp rise at 75 m (Figure 3e). This last observation was likely driven by the assimilation-driven elevation of nitrate $\delta^{15}N$ at 75 m, due to the isotopic fractionation associated with nitrate assimilation by phytoplankton (Fawcett et al., 2015; Knapp et al., 2005). Below this, at ~100 m, $\delta^{15}N_{TDN}$ was on average 4.5 ± 0.2‰ and [TDN] = 14.3 ± 2.4 μM. At stations where the nitracline was shallower, the $\delta^{15}N_{TDN}$ depth structure was also displaced to shallower depths. Below the nitracline, $\delta^{15}N_{TDN}$ increased gradually to 200 m.

3.4. DON Concentration and $\delta^{15}N$

Surface (5 m) water [DON] had a relatively narrow range (4.4–4.9 μM, 4.6 ± 0.1 μM) (Figures 3c and 4a). Relatively higher surface [DON] was observed between 13°N and 14°N and at the southwestern stations. [DON] was generally the highest at the surface and decreased with depth, averaging 4.3 ± 0.2 μM at 50 m and 4.1 ± 0.3 μM at 75 m.

In the surface ocean, DON $\delta^{15}N$ ($\delta^{15}N_{DON}$) averaged 4.3 ± 0.2‰, with lower $\delta^{15}N_{DON}$ generally corresponding to the sites of higher [DON]. Vertically, $\delta^{15}N_{DON}$ generally increased with depth, reaching 4.7 ± 0.2‰ at 50 m (Figures 3f and 4b). At 75 m, $\delta^{15}N_{DON}$ averaged 4.8 ± 0.4‰.

3.5. Suspended PN Concentration and $\delta^{15}N$

The concentration of suspended PN [PN_{susp}] in surface water ranged from 0.11 to 0.41 μM and averaged 0.20 ± 0.07 μM (n = 41) (Figure 5a). Higher [PN_{susp}] was observed in the northwestern and southwestern parts of the sampling region. The $\delta^{15}N$ of suspended PN ($\delta^{15}N_{susp}$) had a range of 1.0–5.2‰ and averaged

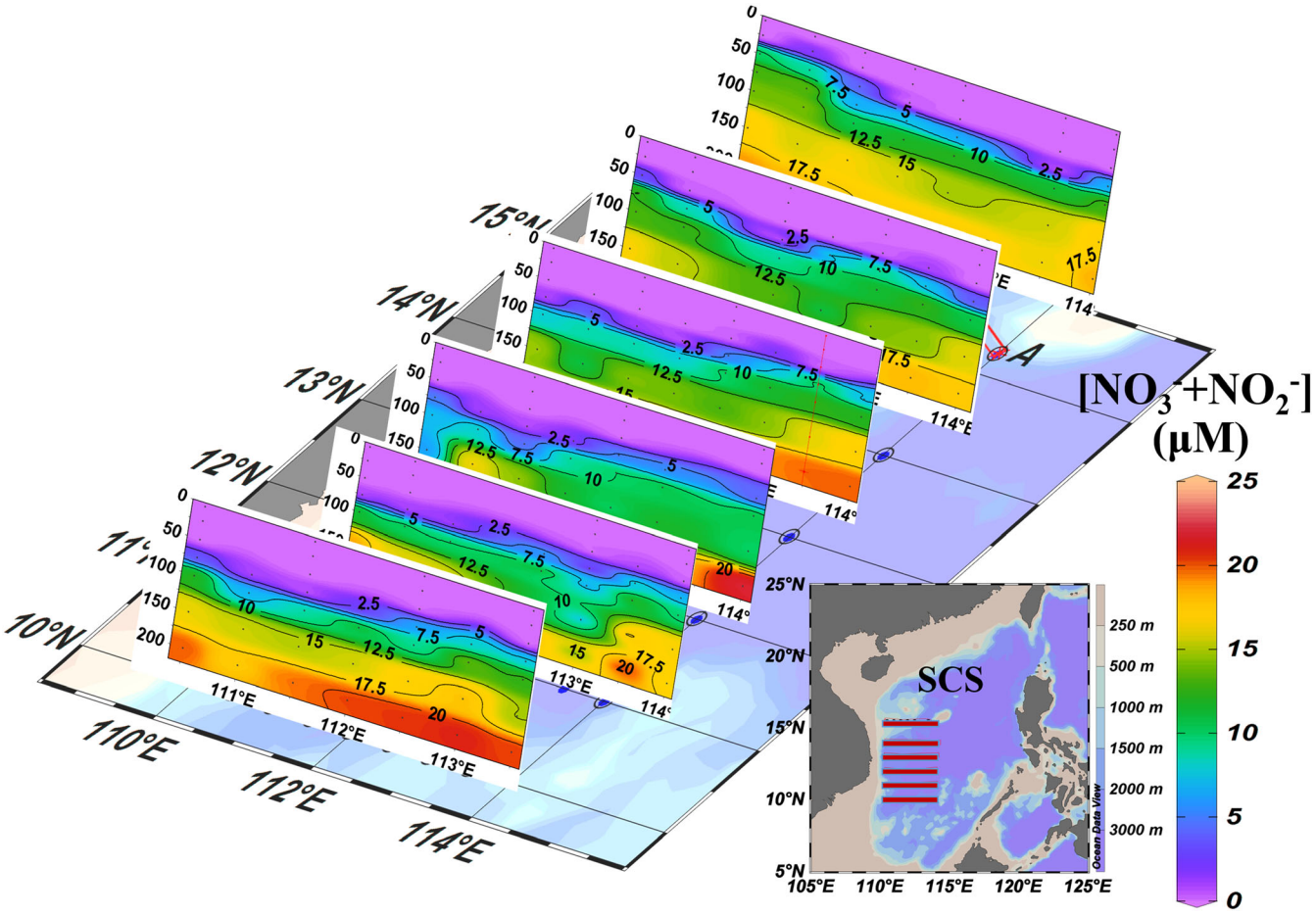

Figure 2. Concentration of nitrate + nitrite ([NO_3^- + NO_2^-]) in the upper 200 m along the six zonal sections (10°N, 11°N, 12°N, 13°N, 14°N, and 15°N) of sampling stations.

2.3 ± 0.9‰ (n = 41) (Figure 5b). Most stations (35 of 41) had a $\delta^{15}N_{susp}$ < 3.0‰. Higher $\delta^{15}N_{susp}$ values were only observed in the northwestern part of sampling region (Stations 60–64, n = 5; mean values for [PN] of 0.31 ± 0.07 μM and for $\delta^{15}N_{susp}$ of 4.2 ± 0.7‰), where the nitracline was shallower. For the majority of sampling stations, in the surface water (5 m), suspended PN $\delta^{15}N$ was ~2‰ (2.1 ± 0.5‰).

4. Discussion

4.1. DON Production in the Surface SCS

[DON] and [PN_{susp}] were the highest at the surface, where primary production in the SCS water column is also the highest (Liu et al., 2007). A positive correlation (r = 0.96, p = 0.01) between DON stock in the upper 50 m and remote-sensed surface chlorophyll a has been observed in the ETSP, which was used to infer net DON production in the local euphotic zone (Knapp et al., 2018). In the SCS, a positive correlation between [DON] and chlorophyll a concentration was also observed in surface waters (Figure 6a; r = 0.65, p = 0.002, n = 19), suggesting surface DON production at these sites as well. However, the intercept of the correlation is 4.2 ± 0.1 μM, suggesting that only a small fraction of the DON in the surface waters was newly produced. In addition, [PN_{susp}] and chlorophyll a also showed a moderate correlation (Figure 6b; r = 0.64, p < 0.001, n = 29) but with an intercept close to zero. This is consistent with the canonical view that suspended PN in the surface waters has a short residence time, such that most surface suspended PN is generated and consumed within the region that it is observed (Sigman & Fripiat, 2019; Waser et al., 2000). Like organic N, both dissolved organic carbon and particulate organic carbon in the euphotic zone have been reported to be well correlated to chlorophyll a in the SCS basin (Hung et al., 2007). The spatial pattern of [DON] agrees broadly

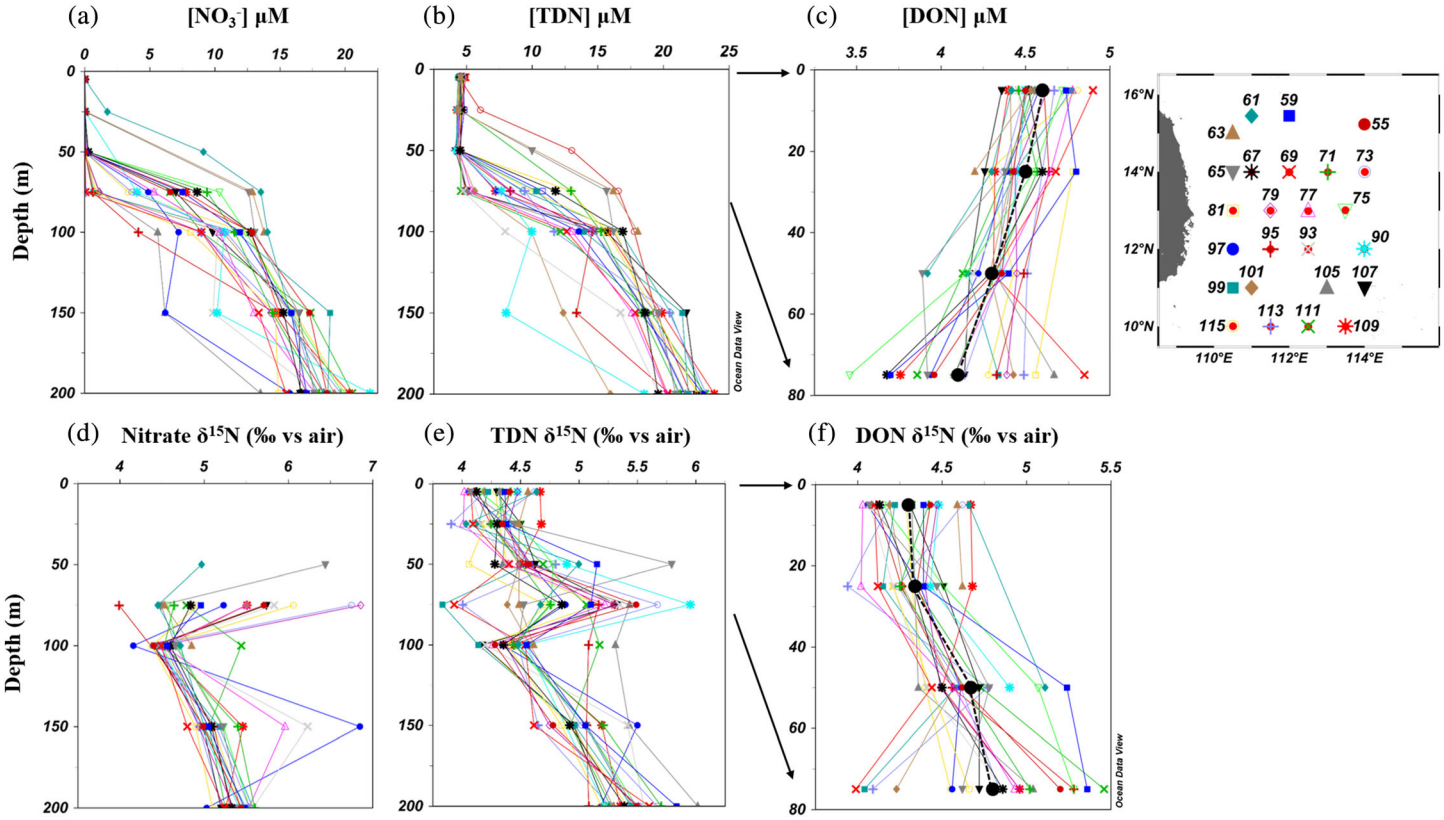

Figure 3. Depth profiles of concentration and $\delta^{15}N$ of different N pools. Panels (a)–(c) are for concentration of nitrate, TDN, and DON, respectively. Panels (d)–(f) are for the isotopic composition of nitrate, TDN, and DON, respectively. TDN and nitrate data are shown in the upper 200 m, while DON data are shown in the upper 75 m. Averages of [DON] and DON $\delta^{15}N$ are shown in black filled circles with dashed lines (panels c and f). Nitrate was depleted, and thus, the corrections for nitrate were insignificant in the upper 50 m, while the interference of nitrate became significant at 75 m.

with prior compilation of global observations that [DON] is coherent with primary productivity in general, with low concentrations of DON in the gyre centers and higher concentrations in areas of upwelling (Letscher et al., 2013).

Anthropogenic atmospheric N (AAN) input via deposition can impact the SCS on annual basis (Kim et al., 2014; Ren, Chen, et al., 2017). However, the existing evidence argues against a major role for atmospheric N deposition in the production of "labile" DON and its $\delta^{15}N_{DON}$ in this study, for following reasons. Multiyear-averaged total aerosol optical thickness from MODIS for each month in the SCS implies that our sampling region (~10–15°N, 110–115°E) received minimal atmospheric deposition during the sampling month (Lin et al., 2007). There are two main sources of terrestrial aerosols to the SCS: the northern source comprised of fossil fuel aerosols from East China and Asian desert (Gobi Desert) and the southern source from biomass burning in Sumatra and Borneo of the Southeast Asia (Lin et al., 2007, 2009). These aerosols are transported by the prevailing NE and SW monsoons, respectively (Lin et al., 2007, 2009). The northern source usually can extend southward to around 15–16°N, while the southern source can extend northward to around 11°N (Lin et al., 2007, 2009), such that our study region (~10–15°N, 110–115°E) sits in an approximate gap between the two sources, and it receives much less atmospheric deposition than the northern SCS. Moreover, the input of aerosols associated with biomass burning in Borneo and Sumatra during the sampling month is also minimal over our sampling region (Lin et al., 2007). Even in the northern SCS, where AAN deposition rate is higher and has been rising since 2000 (~50 mmol m^{-2} yr^{-1} in 2014; Ren, Chen, et al., 2017), this rate can explain only ~3% of primary production (Ren, Chen, et al., 2017). Thus, it is unlikely that the correlation between the [DON] and chlorophyll *a* is caused by AAN deposition.

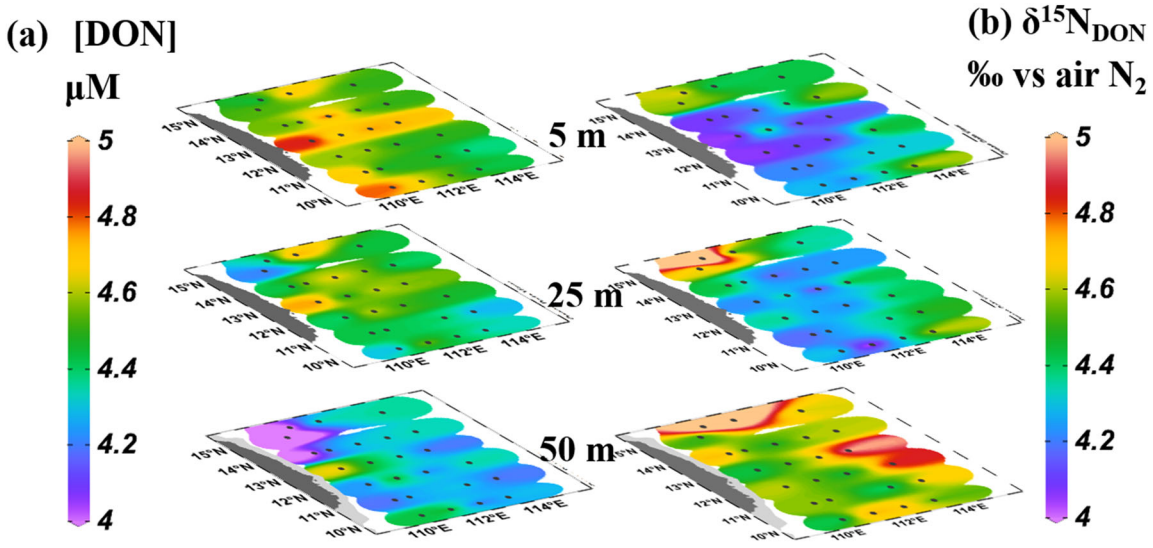

Figure 4. Spatial distributions of [DON] (a) and $\delta^{15}N_{DON}$ (b) at 5, 25, and 50 m.

4.2. DON Consumption With Isotope Fractionation in the Upper Layers

[DON] and $\delta^{15}N_{DON}$ showed a negative correlation ($r = 0.70$; Figure 7a). DON is mainly produced from PN through a range of mechanisms including cell lysis, exudation, and particle solubilization (reviewed in Bronk & Steinberg, 2008, and Sipler & Bronk, 2014), processes that would not be associated with strong isotopic fractionation because they do not specifically attack C-N bonds. Thus, it is expected that "fresh" DON $\delta^{15}N$ should be similar to the $\delta^{15}N$ of PN from which it is produced from (Knapp et al., 2011). This inference is supported by field observations, which show no clear $\delta^{15}N$ elevation in surface detrital PN relative to living PN in the Sargasso Sea (Fawcett et al., 2011). Thus, explanations for DON $\delta^{15}N$ variation in the surface ocean have focused on the isotopic fractionation associated with deamination and similar chemical DON breakdown processes (Knapp et al., 2011, 2012, 2018).

There are two possible explanations for the observed negative correlation: (1) production/addition in WSCS surface waters of DON with a lower $\delta^{15}N$ than that of DON generated in other regions and (2) DON degradation with an isotopic fractionation. The former explanation is unlikely, as mass balance would require the

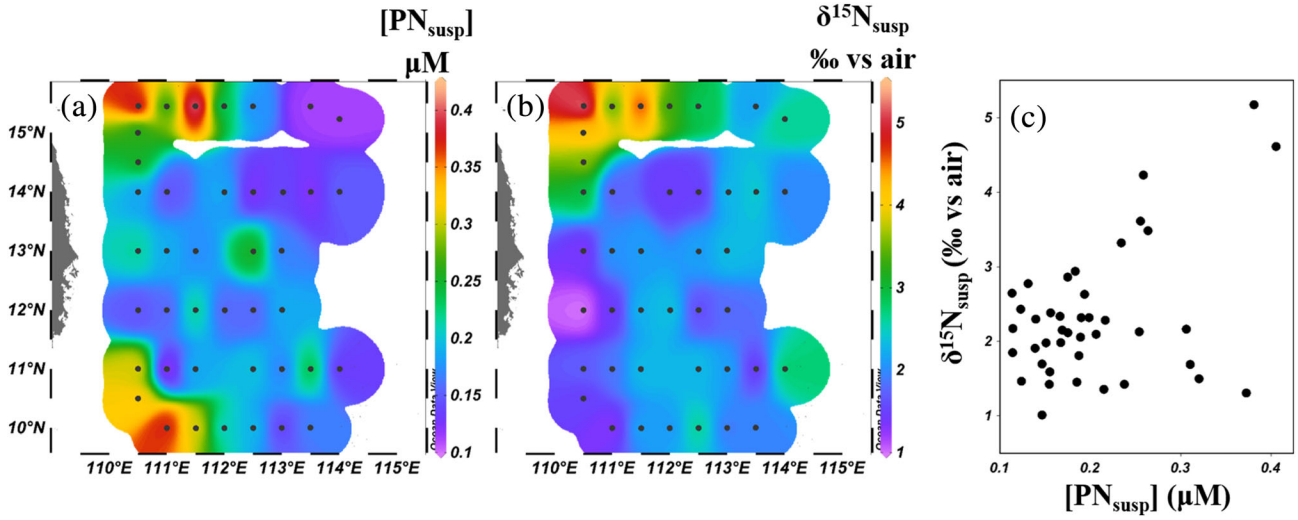

Figure 5. Concentration and $\delta^{15}N$ of suspended PN in surface (5 m) waters (a, $[PN_{susp}]$; b, $\delta^{15}N_{susp}$; c, $\delta^{15}N_{susp}$ vs. $[PN_{susp}]$).

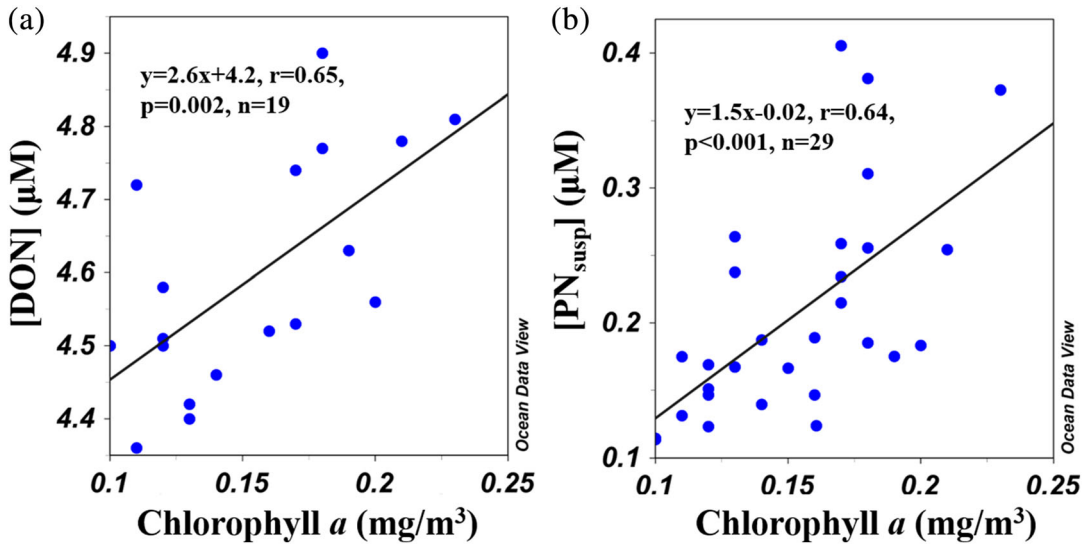

Figure 6. Relationships of [DON] (a) and [PN_{susp}] at 5 m (b) with remotely sensed chlorophyll *a*. The mapped 8 day averaged MODIS chlorophyll *a* data with a 9 km spatial resolution was used. At each sampling station, chlorophyll *a* was calculated by averaging the closest chlorophyll *a* values.

addition of 0.3 μM DON with $\delta^{15}N$ of −1.4‰ in WSCS surface waters. This $\delta^{15}N$ value is far lower than that of subsurface nitrate, the dominant form of fixed N for surface new production (Liu et al., 2010). While it is close to the $\delta^{15}N$ of N_2 fixer biomass and the DON they produce (Carpenter et al., 1997; Macko et al., 1987; McRose et al., 2019; Minagawa & Wada, 1986; Zerkle et al., 2008), we know of no reason to expect N_2 fixers to dominate net DON production in this region. The SCS has relatively strong vertical exchange and net upwelling, with both monsoonal seasons hosting conditions that encourage vertical fluxes (Liu & Gan, 2017). This results in high vertical nitrate flux to the euphotic zone on an annual basis, which dominates new production (Liu et al., 2010; Ren, Chen, et al., 2017). Overall, work to date in the SCS suggests that the rate of N_2

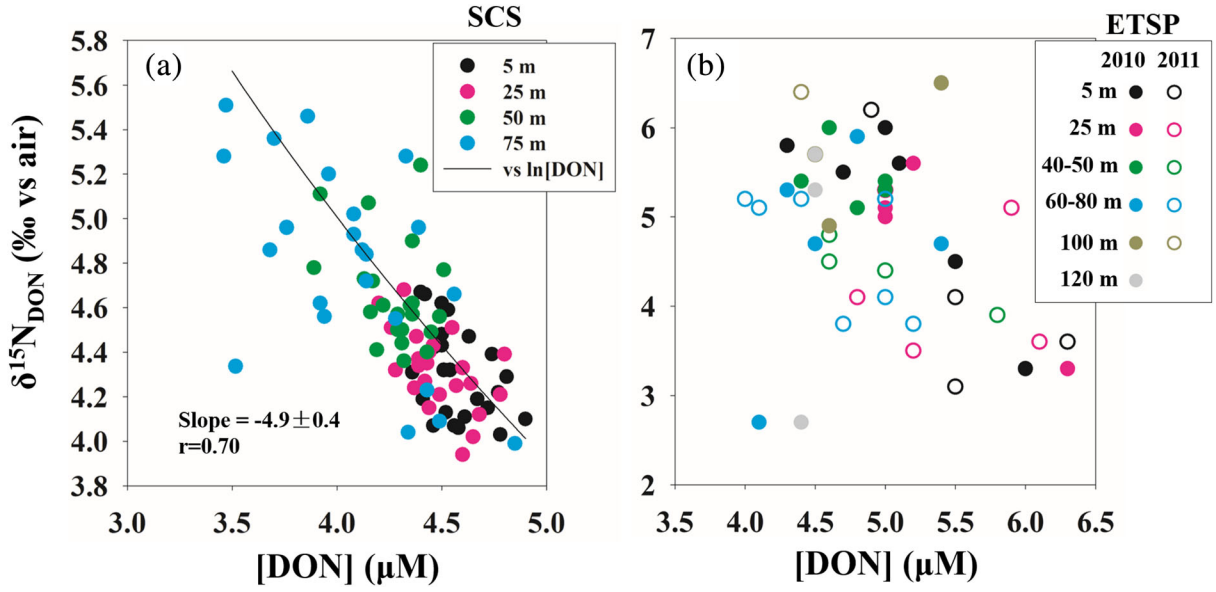

Figure 7. Relationship between $\delta^{15}N_{DON}$ and [DON] in the upper 75 m of the WSCS (a) and in the upper 120 m of the Eastern Tropical South Pacific (ETSP) (b). The ETSP data are from Knapp et al. (2018). In panel (b), data points from 2010 and 2011 cruises are denoted in filled and open circles, respectively. In (a), assuming the Rayleigh model for DON consumption (i.e., irreversible consumption of DON with constant isotopic fractionation in a closed system), the slope of the linear fit of $\delta^{15}N_{DON}$ against ln[DON] provides an estimate of isotope effect (ε) for DON consumption of 4.9 ± 0.4‰.

fixation is low relative to the vertical nitrate flux (~20 mmol N m^{-2} yr^{-1} vs. 200 mmol N m^{-2} yr^{-1}), based on multiple lines of evidence including bottle incubations, natural-abundance nitrogen isotope analyses, genetic analysis, and biogeochemical modeling (Chen et al., 2014, 2008; Kao et al., 2012; Liu et al., 2010; Lu et al., 2019; Ren, Chen, et al., 2017; Shiozaki et al., 2014; Voss et al., 2006; Wang et al., 2019; Wong et al., 2007; Yang et al., 2017; Zhang et al., 2015, 2011). It remains possible that N_2 fixation is channeled directly to DON, focusing its isotopic impact on the DON pool. However, the existing data from other regions show no sign of such a connection (Knapp et al., 2012).

Pursuing the second possibility and applying the Rayleigh model (i.e., a closed system with irreversible consumption occurring with a constant isotopic fractionation), an isotope effect (ε) of ~4.9 ± 0.4‰ during DON consumption was calculated (Figure 7a). In the ETSP, a negative correlation ($r = 0.64$, $p = 0.53$) between [DON] and $\delta^{15}N_{DON}$ was also observed in the upper 50 m (Figure 7b), yielding an ε of 5.5 ± 1.2‰ for DON degradation (Knapp et al., 2018), which is similar to the value estimated here, considering the uncertainties. Moreover, an ε of ~3–5‰ for DON degradation has been estimated from data near Station ALOHA in the subtropical North Pacific and the Sargasso Sea (Knapp et al., 2011). The origins of this isotopic fractionation are likely the hydrolysis and deamination of protein, in which there is preferential loss of low-$\delta^{15}N$ amino groups (Bada et al., 1989; Macko et al., 1986; Silfer et al., 1992).

As the concentration of DON is much higher than that of DIN in the surface ocean, even a proportionally small amount of DON degradation may represent an important source of recycled N to the surface ocean. DON degradation may release bioavailable N in the forms of simple organic N compounds and ammonium, which can be directly and rapidly assimilated (Sipler & Bronk, 2014). Since DON degradation appears to release N with a low $\delta^{15}N$, it should have influenced the $\delta^{15}N$ of the PN_{susp} pool, a large fraction of which can be viewed as short-term accumulated fresh photosynthetic products. Indeed, low-surface $\delta^{15}N_{susp}$ (2.3‰) was observed during our sampling period (Figure 5b), consistent with the contribution of N with a low $\delta^{15}N$ from DON degradation.

The upper 50 m of the SCS basin represents a N-depleted layer, with nitrate + nitrite or ammonium near detection limits (Du et al., 2017). Any allochthonous N sources, either as DIN or degradable DON, would help relieve the N deficiency in the euphotic zone. Our interpretation suggests that some portion of DON in the SCS is degradable, supporting the importance of DON consumption in the upper ocean nitrogen cycle.

4.3. DON and the Subsurface $\delta^{15}N_{NO3}$ Minimum

The presence of a shallow subsurface $\delta^{15}N_{NO3}$ minimum is ubiquitous in low-latitude oligotrophic oceans (Casciotti et al., 2008; Knapp et al., 2005; Liu et al., 1996). In the WSCS, we also observed a $\delta^{15}N_{NO3}$ minimum (4.6‰) at most stations at ~100 m (Figures 3d and 8). This $\delta^{15}N_{NO3}$ minimum value from the WSCS is identical, within error, to those reported in other regions of the SCS (~4.8‰ at 18–22°N, Ren, Sigman, et al., 2017; Yang et al., 2017, and ~4.7‰ at 12–20°N, Yang et al., 2018), indicating spatial and temporal persistence of the $\delta^{15}N_{NO3}$ minimum in the SCS and arguing for a basin-wide process as its cause.

The subsurface $\delta^{15}N_{NO3}$ minimum in oligotrophic regions has been suggested to result from an addition of isotopically light N to the surface ocean ecosystem (e.g., N_2 fixation) (Casciotti et al., 2008; Knapp et al., 2005, 2008; Lehmann et al., 2018; Liu et al., 1996; Yang et al., 2017). This interpretation may at first appear contradictory to the evidence that these fluxes are low relative to the upward nitrate supply to the euphotic zone, as discussed above (e.g., Kao et al., 2012; Liu et al., 2010; Zhang et al., 2015). However, the N budget of the euphotic zone should be differentiated from that of the thermocline and above. The N in the euphotic zone has a short residence time, with most of the N being supplied from below and exported within a year; in this context, N_2 fixation and atmospheric N deposition are less important additional fluxes. In contrast, the residence time of fixed N in thermocline is longer, allowing the isotopic signals of N_2 fixation and atmospheric N deposition to accumulate over multiple years. This explains why N_2 fixation changes have been identified in studies of foraminifera-bound N (Ren, Sigman, et al., 2017) even though these fluxes represent the minority of the fixed N being supplied to the euphotic zone in any given year.

It should be noted that the signal of low-$\delta^{15}N$ N from N_2 fixation or atmospheric deposition cannot impact the subsurface $\delta^{15}N_{NO3}$ directly, as any added DIN would be consumed in the upper euphotic zone before it can reach the subsurface. Rather, it should be the downward transport and remineralization of organic N

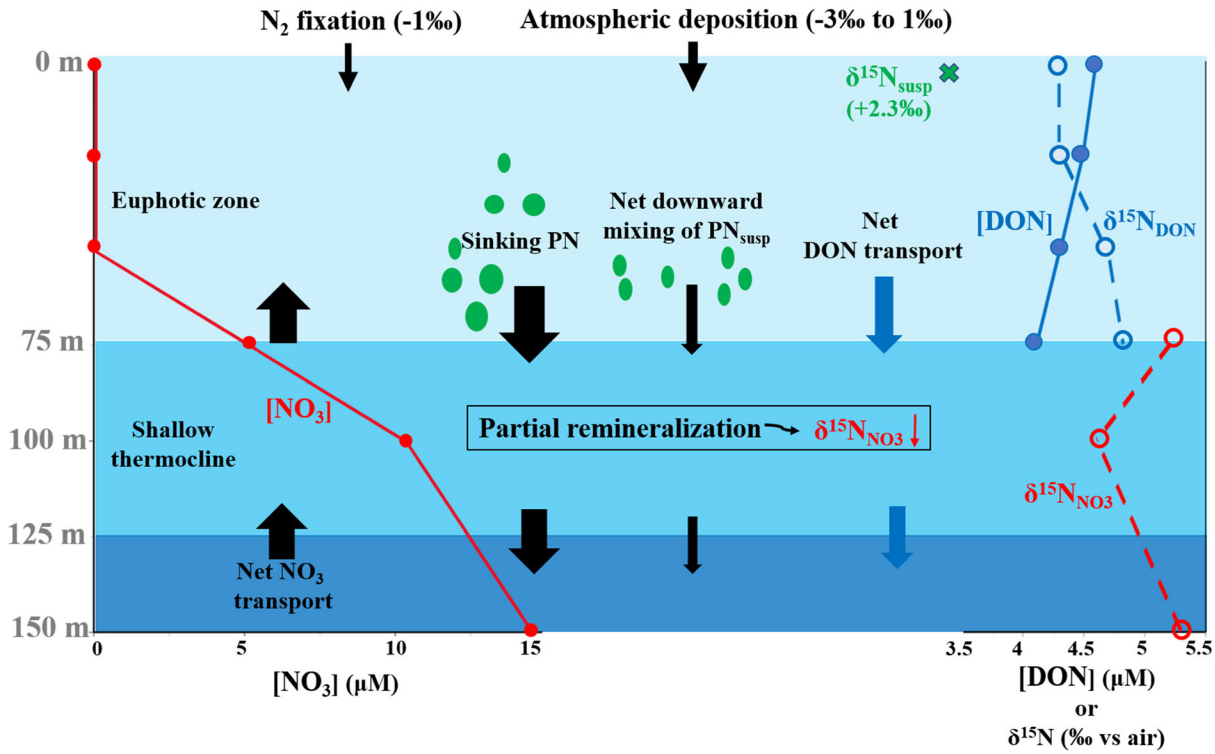

Figure 8. Schematic of the N fluxes in the upper water column of the SCS basin. Depth profiles of nitrate concentration, DON concentration, nitrate $\delta^{15}N$, and DON $\delta^{15}N$ are also shown, based on calculations from the data reported here. The depth range 0–75 m roughly represents the euphotic zone in the SCS basin. It should be noted that the arrows for nitrate, DON, and downward mixing of suspended PN all represent net (not gross) fluxes. Riverine input of N is minimal for the open water stations (Cai et al. 2004) and is not shown. The $\delta^{15}N$ range of atmospheric N deposition is from Yang et al. (2014) and Xiao et al. (2018). These values are based on measurements of deposition and do not correct for any N deposition with a local marine origin (Altieri et al., 2016). $\delta^{15}N$ of N_2 fixation product is from Montoya et al. (2002).

derived from N_2 fixation or atmosphere deposition that communicates the low-$\delta^{15}N$ signal to the subsurface nitrate pool. The importance of DON relative to PON in downward transport and remineralization is not well known, and the N isotopes may provide new constraints.

Another important question is whether the $\delta^{15}N$ lowering of the thermocline nitrate relative to deeper nitrate requires N_2 fixation and atmospheric N deposition, the alternative being that it derives solely from fractionation during partial remineralization of organic N being exported from the euphotic zone. This question is important, for example, in the effort to reconstruct past changes in N_2 fixation and/or atmospheric N deposition. Below consider in turn the N pools and fluxes that might work to generate the nitrate $\delta^{15}N$ minimum without requiring any input of low-$\delta^{15}N$ newly fixed N to the euphotic zone.

The suspended PN in surface waters has a low $\delta^{15}N$ (~2‰ lower than the $\delta^{15}N$ of the nitrate supply in the SCS), probably due to the preferential remineralization of ^{14}N into ammonium that is then assimilated into the phytoplankton pool (Altabet, 1988; Checkley & Entzeroth, 1985; Checkley & Miller, 1989; Fawcett et al., 2011, 2015; Treibergs et al., 2014). This implies that a complementarily higher $\delta^{15}N$ N is exported as sinking N (fecal pellets, etc.) (Altabet, 1988; Altabet & Small, 1990). A portion of the sinking N penetrates deeply into the ocean interior before being remineralized. In contrast, the low-$\delta^{15}N$ suspended PN can only be mixed downward before remineralization. The $\delta^{15}N$ difference between sinking and suspended PN thus effectively concentrates ^{14}N in the upper ocean (including the shallow subsurface) relative to the deeper ocean and may contribute to lowering the $\delta^{15}N$ of shallow thermocline nitrate. However, this process is probably a minor contributor to the $\delta^{15}N_{NO3}$ minimum (Knapp et al., 2005), as surface [PN_{susp}] is low (<0.2 μM in this study), such that only small amounts of PN are available to be mixed down into the shallow subsurface and then remineralized.

Fractionation during remineralization of sinking PN represents a second process that might, by itself, lower the $\delta^{15}N$ of thermocline nitrate, by preferentially releasing low-$\delta^{15}N$ ammonium into the shallow subsurface. It would be easy for this process to lower the $\delta^{15}N$ of shallow subsurface nitrate, as the sinking flux of PN is the dominant mechanism by which N is transferred from the surface to the subsurface. However, there is not clear evidence for isotopic fractionation (preferential loss of ^{14}N relative to ^{15}N) associated with N loss during sinking. Yang et al. (2017) reported sinking PN $\delta^{15}N$ to be 4.9‰ at 100 m and 3.3‰ at 150 m by floating trap in the SCS basin (18°N), implying a decreasing trend of sinking PN $\delta^{15}N$ with depth in the upper water column of the SCS. Over a greater depth range, prior studies have found that the $\delta^{15}N$ of sinking PN generally decreases with depth in the North Atlantic (Altabet et al., 1991). Thus, while the remineralization of low-$\delta^{15}N$ sinking PN would work to lower the $\delta^{15}N$ of the shallow thermocline nitrate, it does not appear that isotopic fractionation during the remineralization of sinking PN is the cause.

Given the focus of our study on DON, we are motivated to ask whether isotopic fractionation during degradation of DON as it is mixed downward might explain or contribute to the shallow subsurface $\delta^{15}N_{NO3}$ minimum (Figure 8). Fractionation during DON remineralization contributing to nitrate $\delta^{15}N$ minimum would need to rely on the downward mixing of DON also occurring in waters below ~100 m depth, with the residual high-$\delta^{15}N$ DON escaping into deeper layers. This is plausible, as the vertical gradients of [DON] (Figure 3) could support a flux of DON out of the euphotic zone and into waters below ~125 m (Abell et al., 2000). In this way, isotopic fractionation during the degradation of DON as it is mixed downward would preferentially add ^{14}N-rich nitrate into the shallow subsurface.

This last mechanism should be evidenced by an increase in DON $\delta^{15}N$ with increasing depth that accompanies the commonly observed decline in DON concentration with depth. In this regard, the data are ambiguous. In the Sargasso Sea, Knapp et al. (2005) observed an increase in total organic nitrogen (TON = DON + PN_{susp}) $\delta^{15}N$ with depth but found that most of that increase could be explained by suspended PN changes. Near Hawaii, Knapp et al. (2011) reconstructed a decline in TON $\delta^{15}N$ with depth, a sense of change that contradicts the expectations above. In the SCS data reported here, a downward increase in DON $\delta^{15}N$ is observed down to 75 m (Figure 3f), but the data do not speak to deeper levels. To advance this question further, approaches are needed to measure the bulk DON $\delta^{15}N$ in samples with high DIN concentration.

4.4. The Shallow Subsurface Nitrate $\delta^{15}N$ Minimum in the SCS: Comparison With Other Subtropical Regions

The value of the shallow subsurface $\delta^{15}N_{NO3}$ in the SCS (4.6 ± 0.2‰) is higher than that reported in the adjacent West Philippine Sea (~2‰) at a similar potential density surface (Yang et al., 2017), near Hawaiian Ocean Time series (HOT) in the subtropical North Pacific (~4‰) (Casciotti et al., 2008; Knapp et al., 2011; Sigman et al., 2009) and Bermuda Atlantic Time series Site (BATS) (~2.5‰) (Fawcett et al., 2015; Knapp et al., 2005). Conceptually, the magnitude of the shallow subsurface $\delta^{15}N_{NO3}$ minimum should be the net result of the input of N to the upper ocean that is lower in $\delta^{15}N$ than that of the nitrate supply from below (e.g., from the deeper thermocline). With regard to the latter, the SCS has distinct characteristics compared to the subtropical gyres. The SCS is a region of strong vertical exchange and net upwelling, with both monsoonal seasons hosting conditions that encourage vertical fluxes (Liu & Gan, 2017). This relatively rapid gross input of nitrate from below may contribute to the observation of a weaker decline in the $\delta^{15}N$ of nitrate from the deep ocean to the shallow thermocline of the SCS.

The nitrate concentrations between 150 and 300 m in the SCS are much higher than that observed at other subtropical regions such as HOT and BATS (Figure 9), which suggests that the supply rate of nitrate from below to this layer is higher in the SCS. This is consistent with the previously estimated short residence time of water in the shallow subsurface (~3 yr) in the SCS (Liu & Gan, 2017). This suggests that an isotopic distinction between the nitrate above and below 150 m has much less time to develop in the SCS than in other subtropical ocean regions. For example, the residence time of nitrate in the comparable shallow subsurface layer at HOT is ~25 yr (Casciotti et al., 2008). Due to a short residence time of the shallow subsurface nitrate at the depths of the $\delta^{15}N_{NO3}$ minimum, the amount of organic matter (DON or sinking PN) decomposition in the water column is insufficient to produce a $\delta^{15}N_{NO3}$ minimum as strong as that observed elsewhere (e.g., at BATS). Moreover, the net upwelling leads to shallow thermocline nitrate concentrations in the SCS that

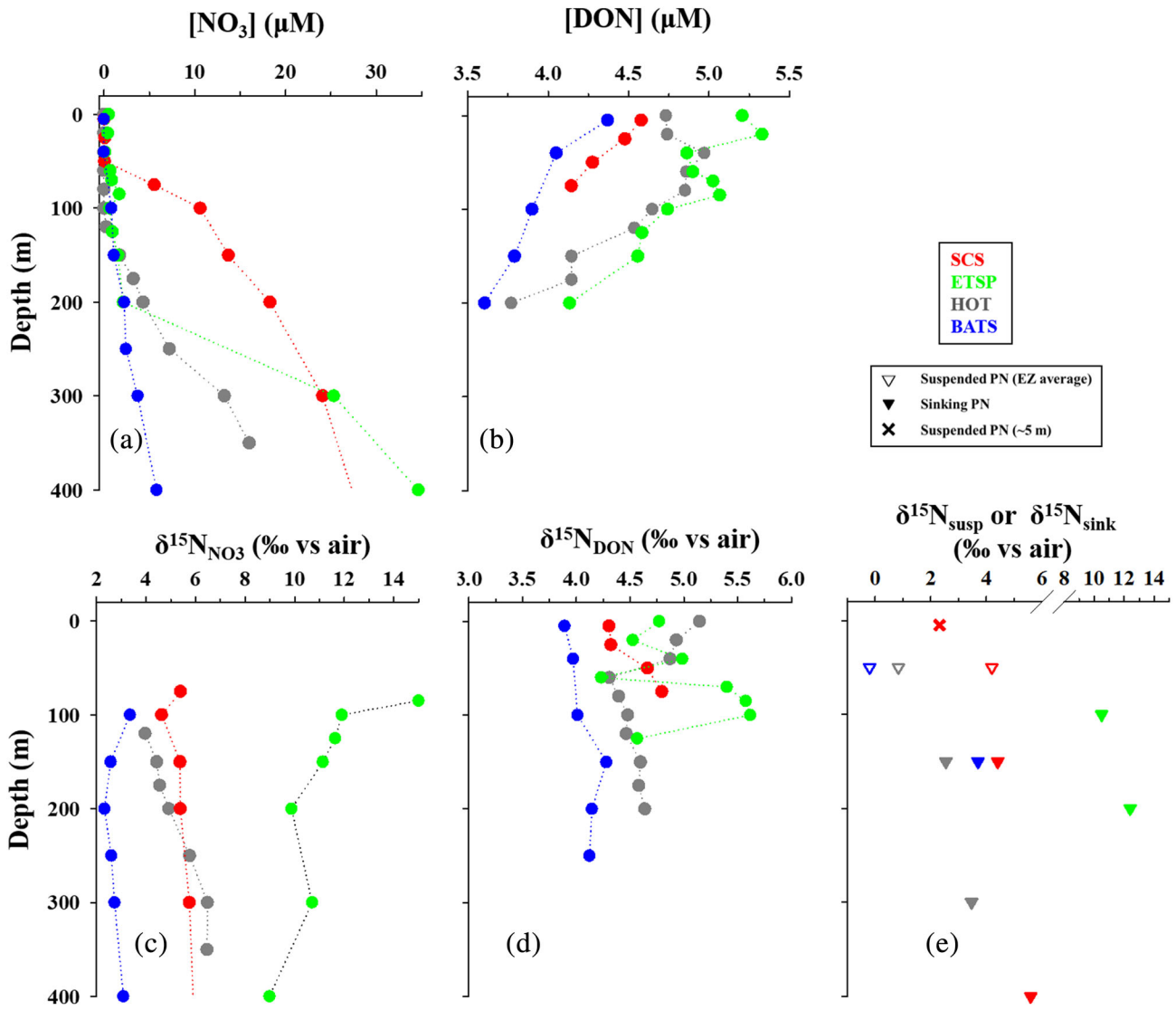

Figure 9. Depth profiles of [NO_3^-] (a), [DON] (b), $\delta^{15}N$ of nitrate (c), $\delta^{15}N$ of DON (d), and $\delta^{15}N$ of suspended PN and sinking PN in four regions (SCS, ETSP, HOT, and BATS) (e). Mean values are used. BATS data are from Knapp et al. (2005). HOT data are from Casciotti et al. (2008) and Knapp et al. (2011). ETSP data are from Knapp et al. (2016) and Knapp et al. (2018). The SCS euphotic zone mean $\delta^{15}N$ of suspended PN ($\delta^{15}N_{susp}$), $\delta^{15}N$ of shallow sinking PN ($\delta^{15}N_{sink}$), and $\delta^{15}N_{sink}$ at 200 m data are from Yang et al. (2017). SCS [NO_3^-], [DON], $\delta^{15}N_{NO3}$, $\delta^{15}N_{DON}$, and surface (5 m) $\delta^{15}N_{susp}$ data are from this study.

are much higher than in the subtropical gyres, such that the isotopic signal of any low-$\delta^{15}N$ N addition from above is diluted by the abundance of nitrate supplied from below. These considerations currently represent the best explanation for the observation that the shallow thermocline nitrate $\delta^{15}N$ minimum is weaker than in other oligotrophic waters.

4.5. Net Production and Consumption of DON: A Global Comparison

Regional variations in the $\delta^{15}N_{DON}$ have also been identified. Knapp et al. (2011) measured a ~1‰ difference in euphotic zone DON $\delta^{15}N$ between BATS in the North Atlantic and the HOT site in the North Pacific, which was interpreted as originating from the different subsurface nitrate $\delta^{15}N$ between the regions of the two sites. We compare our data from the SCS with the BATS and HOT results and with recent measurements from the ETSP.

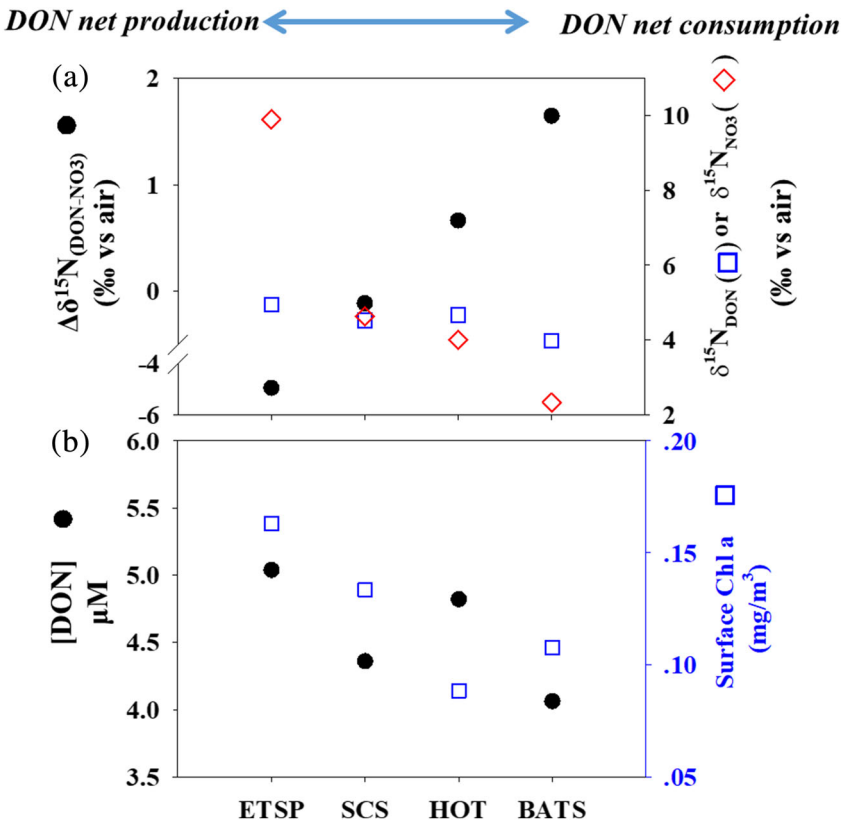

Figure 10. Comparison of $\Delta\delta^{15}N_{(DON\text{-}NO3)}$ (=euphotic zone $\delta^{15}N_{DON}$ − shallow subsurface $\delta^{15}N_{NO3}$), euphotic zone $\delta^{15}N_{DON}$ and shallow subsurface $\delta^{15}N_{NO3}$ (a), and [DON] and surface chlorophyll *a* concentration in four regions (ETSP, SCS, HOT, and BATS) (b). Mean values for each parameter were used. BATS [DON] and $\delta^{15}N$ data are from Knapp et al. (2005). HOT [DON] and $\delta^{15}N$ data are from Casciotti et al. (2008) and Knapp et al. (2011). ETSP [DON] and $\delta^{15}N$ data are from Knapp et al. (2016) and Knapp et al. (2018). Chlorophyll *a* data for ETSP and SCS were obtained from MODIS multiyear mean (2002–2015). Mean values for chlorophyll *a* at HOT and BATS are from Karl and Church (2017) and Saba et al. (2010), respectively.

As shown in Figure 9, [DON] and $\delta^{15}N_{DON}$ in the WSCS fall in the reported range in the low-latitude waters. The ETSP has both the highest [DON] and $\delta^{15}N_{NO3}$ among the four regions, due to the influence of higher productivity and water-column denitrification in the eastern Pacific (Deutsch et al., 2001; Pennington et al., 2006) and the associated isotopic fractionation leaving the residual nitrate pool enriched in ^{15}N (Brandes et al., 1998; Liu & Kaplan, 1989). [DON] in the upper 75 m of the WSCS is close to the global mean surface DON concentration, ~4.4 ± 0.5 μM (Letscher et al., 2013). [DON] shows a similar decline with depth through the upper water column in all four regions (Figure 9b). In contrast, the $\delta^{15}N_{DON}$ variation with depth is not consistent among the four regions, implying a different set of influences on DON $\delta^{15}N$ (Figure 9c).

The difference between the $\delta^{15}N$ of euphotic zone DON and shallow subsurface nitrate ($\Delta\delta^{15}N_{(DON\text{-}NO3)} = \delta^{15}N_{DON} - \delta^{15}N_{NO3}$) is a potentially useful property. $\Delta\delta^{15}N_{(DON\text{-}NO3)}$ in the four regions are as follows, listed in order from lowest to highest: ETSP (−4.9 ± 0.4‰), SCS (−0.1 ± 0.4‰), HOT (0.7 ± 0.2‰), and BATS (1.6 ± 0.5‰). As revealed by prior studies and supported by our results, nitrate upwelled from the shallow subsurface is the main N source for DON formation in the upper ocean (Knapp et al., 2005, 2011; Yamaguchi & McCarthy, 2018). The newly produced autochthonous DON should have a $\delta^{15}N$ similar to its PN source (Knapp et al., 2005), while DON consumption generally makes residual DON more enriched in ^{15}N (Knapp et al., 2018, and this study). Since euphotic zone PN_{susp} $\delta^{15}N$ is typically lower than the $\delta^{15}N$ of the nitrate supply from below, in the case of DON production but minimal DON consumption

(net production), $\Delta\delta^{15}N_{(DON\text{-}NO3)}$ should tend to be low and possibly negative. In the case of net DON consumption, $\Delta\delta^{15}N_{(DON\text{-}NO3)}$ should tend toward higher values. Thus, we propose that this pattern reflects variations among the regions in whether they are characterized by net production or consumption of DON, with net DON production in the more eutrophic ETSP and net DON consumption in more oligotrophic subtropical gyres in the North Pacific and North Atlantic (Figure 10a). Notably, $\Delta\delta^{15}N_{(DON\text{-}NO3)}$ is intermediate (close to zero) in the SCS, suggesting a near equivalence in DON production and consumption in the SCS euphotic zone. Two lines of evidence are consistent with this overarching interpretation. First, chlorophyll *a* varies across the sites as would be expected for ETSP to be the region of net DON production and HOT and BATS to characterize regions of net DON consumption (Figure 10b). Second, this same pattern in DON production and consumption has been found from analysis of DON concentration data (Letscher et al., 2013).

One obvious flaw in this analysis relates most strongly to the ETSP. The region is characterized by rapid lateral flows at the surface (Kessler, 2006) and strong spatial gradients in nitrate $\delta^{15}N$ in the shallow subsurface (Peters et al., 2018). Moreover, DON can be transported at basin scale by circulation (Letscher et al., 2013; Letscher et al., 2016; Torres-Valdés et al., 2009), which tends to homogenize the isotopic composition of the oceanic DON pool. Thus, in the ETSP, the shallow subsurface nitrate $\delta^{15}N$ cannot be taken as accurately reflecting the $\delta^{15}N$ of the nitrate supply that fueled the DON produced in the surface waters (Knapp et al., 2018), potentially explaining the high amplitude negative value of $\Delta\delta^{15}N_{(DON\text{-}NO3)}$ in the ETSP.

In addition, these considerations point to the persistence and circulation of DON in surface waters as a broad alternative explanation for the observed pattern in $\Delta\delta^{15}N_{(DON\text{-}NO3)}$. If there is an adequately long-lived portion of DON in surface waters, its widespread circulation would tend to homogenize the $\delta^{15}N$ of bulk DON across the surface waters of the global ocean. In this case, the $\delta^{15}N$ of bulk DON in the surface ocean would vary less than the $\delta^{15}N$ of shallow subsurface nitrate, as observed (Figure 10a). The relative importance of this explanation relative to the explanation involving net production/consumption can be addressed with measurements from as-yet unstudied regions.

5. Conclusions

In this study, we present the first data set of DON isotopic composition ($\delta^{15}N$) from the SCS, the largest marginal sea in the western Pacific. A positive correlation between the concentration of DON in the surface ocean and chlorophyll *a* concentration suggests DON production in these surface waters. As in other oligotrophic ocean regions, the concentration and $\delta^{15}N$ of DON fall in a relatively narrow range. DON shallower than 50 m has a mean $\delta^{15}N$ value (4.5‰) that is close to that of subsurface nitrate (4.6‰) but higher than the $\delta^{15}N$ of surface ocean suspended particles (2.3‰), implying the cycling of N among PON, DON, and ammonium in which DON degradation occurs with isotopic fractionation. A negative correlation ($r = 0.70$) between [DON] and DON $\delta^{15}N$ was observed in the upper 75 m, indicating an isotope effect for DON degradation of ~4.9‰, consistent with findings from elsewhere. Comparing the SCS data with those from three other regions, we propose that the $\delta^{15}N$ difference between euphotic zone DON and shallow subsurface nitrate $\delta^{15}N$ ($\Delta\delta^{15}N_{(DON\text{-}NO3)}$) reflects the balance between net DON production or consumption. Specifically, $\Delta\delta^{15}N_{(DON\text{-}NO3)}$ appears to rise from regions of inferred net DON production (e.g., the ETSP) to regions of net DON consumption (the subtropical gyres of the North Atlantic and North Pacific), with the SCS representing an intermediate case. An additional possible contributor to the pattern in $\Delta\delta^{15}N_{(DON\text{-}NO3)}$ is that there is a long-lived portion of DON, the widespread circulation of which homogenizes the $\delta^{15}N$ of bulk DON across the surface waters of the global ocean. In this case, the $\delta^{15}N$ of bulk DON in the surface ocean would vary less than the $\delta^{15}N$ of shallow subsurface nitrate. The relative importance of these two explanations can be addressed with additional measurement campaigns from as-yet unstudied regions.

Our findings provide additional support for the possibility that DON plays an important role in the upper ocean N cycle. Lateral transport of DON from regions of net production (such as basin margins and upwelling areas) potentially influences the nutrient balance in the more oligotrophic and stratified tropical and subtropical basin interior. More spatially extensive N isotopic data sets for DON, complementing the grow-

ing data on DON concentrations, may clarify the importance of such long-distance lateral connections among ocean regions with distinct biogeochemical conditions (Letscher et al., 2013).

Data Availability Statement

Surface chlorophyll *a* concentration was taken from the Moderate Resolution Imaging Spectroradiometer (MODIS; https://oceandata.sci.gsfc.nasa.gov/MODIS-Aqua). Other data for this study are available online through Mendeley Data (https://data.mendeley.com/datasets/7k53k4nzc7/draft?a=b91ee88f-5355-4d64-ae04-080ac2955265).

Acknowledgments

This work was supported by the National Nature Science Foundation of China (42076042, 41721005, 41676174), China Ministry of Science and Technology (2017FY201403), the Foundation of China Ocean Mineral Resources R&D Association (DY135-E2-2-03), and China Scholarship Council. D. M. S. and the isotopic analysis facilities at Princeton were supported by the U.S. NSF through grant OCE-0960802 to D. M. S. and grant OCE-1136345 to B. B. Ward and D. M. S.; support was also provided by the Grand Challenges Program of Princeton University. Samples were collected onboard R/V "*SHIYAN 3*" implementing the open research cruise NORC2015-07 supported by NSFC Shiptime Sharing Project. Thanks are due to M. Zheng, Y. Qiu, X. J. Wang, S. Chen, and D. Li for help of sampling and measurements. We would like to thank W. Zhuang, X. Liu, and X. L. Li for constructive discussions. The manuscript benifited from the comments raised by the reviewers and editor. The software Ocean Data View was used for making plots (Schlitzer, R., Ocean Data View, https://odv.awi.de, 2018).

References

Abell, J., Emerson, S., & Renaud, P. (2000). Distributions of TOP, TON and TOC in the North Pacific Subtropical Gyre: Implications for nutrient supply in the surface ocean and remineralization in the upper thermocline. *Journal of Marine Research*, *58*, 203–222. https://doi.org/10.1357/002224000321511142

Altabet, M. A. (1988). Variations in nitrogen isotopic composition between sinking and suspended particles: Implications for nitrogen cycling and particle transformation in the open ocean. *Deep Sea Research Part A*, *35*, 535–554. https://doi.org/10.1016/0198-0149(88)90130-6

Altabet, M. A., Deuser, W. G., Honjo, S., & Stienen, C. (1991). Seasonal and depth-related changes in the source of sinking particles in the North Atlantic. *Nature*, *354*, 136–139. https://doi.org/10.1038/354136a0

Altabet, M. A., & Small, L. F. (1990). Nitrogen isotopic ratios in fecal pellets produced by marine zooplankton. *Geochimica et Cosmochimica Acta*, *54*, 155–163. https://doi.org/10.1016/0016-7037(90)90203-W

Altieri, K. E., Fawcett, S. E., Peters, A. J., Sigman, D. M., & Hastings, M. G. (2016). Marine biogenic source of atmospheric organic nitrogen in the subtropical North Atlantic. *Proceedings of the National Academy of Sciences*, *113*(4), 925–930. https://doi.org/10.1073/pnas.1516847113

Bada, J. L., Schoeninger, M. J., & Schimmelmann, A. (1989). Isotopic fractionation during peptide bond hydrolysis. *Geochimica et Cosmochimica Acta*, *53*, 3337–3341. https://doi.org/10.1016/0016-7037(89)90114-2

Benner, R., Biddanda, B., Black, B., & Mccarthy, M. (1997). Abundance, size distribution, and stable carbon and nitrogen isotopic compositions of marine organic matter isolated by tangential-flow ultrafiltration. *Marine Chemistry*, *57*, 243–263. https://doi.org/10.1016/S0304-4203(97)00013-3

Braman, R. S., & Hendrix, S. A. (1989). Nanogram nitrite and nitrate determination in environmental and biological materials by vanadium (III) reduction with chemiluminescence detection. *Analytical Chemistry*, *61*(24), 2715–2718. https://doi.org/10.1021/ac00199a007

Brandes, J. A., Devol, A. H., Yoshinari, T., Jayakumar, D. A., & Naqvi, S. W. A. (1998). Isotopic composition of nitrate in the central Arabian Sea and eastern tropical North Pacific: A tracer for mixing and nitrogen cycles. *Limnology and Oceanography*, *43*, 1680–1689. https://doi.org/10.4319/lo.1998.43.7.1680

Bronk, D. A., See, J. H., Bradley, P., & Killberg, L. (2007). DON as a source of bioavailable nitrogen for phytoplankton. *Biogeosciences*, *4*, 283–296. https://doi.org/10.5194/bg-4-283-2007

Bronk, D. A., & Steinberg, D. K. (2008). Nitrogen regeneration. In D. G. Capone, D. A. Bronk, M. R. Mulholland, & E. J. Carpenter (Eds.), *Nitrogen in the marine environment* (2nd ed., pp. 385–467). San Diego: Elsevier.

Cai, W.-J., Dai, M., Wang, Y., Zhai, W., Huang, T., Chen, S., et al. (2004). The biogeochemistry of inorganic carbon and nutrients in the Pearl River estuary and the adjacent Northern South China Sea. *Continental Shelf Research*, *24*(12), 1301–1319. https://doi.org/10.1016/j.csr.2004.04.005

Carpenter, E. J., Harvey, H. R., Fry, B., & Capone, D. G. (1997). Biogeochemical tracers of the marine cyanobacterium *Trichodesmium*. *Deep Sea Research Part I: Oceanographic Research Papers*, *44*, 27–38. https://doi.org/10.1016/S0967-0637(96)00091-X

Casciotti, K. L., Trull, T. W., Glover, D. M., & Davies, D. (2008). Constraints on nitrogen cycling at the subtropical North Pacific Station ALOHA from isotopic measurements of nitrate and particulate nitrogen. *Deep Sea Research, Part II*, *55*, 1661–1672. https://doi.org/10.1016/j.dsr2.2008.04.017

Checkley, D. M., & Entzeroth, L. C. (1985). Elemental and isotopic fractionation of carbon and nitrogen by marine, planktonic copepods and implications to the marine nitrogen cycle. *Journal of Plankton Research*, *7*, 553–568. https://doi.org/10.1093/plankt/7.4.553

Checkley, D. M., & Miller, C. A. (1989). Nitrogen isotope fractionation by oceanic zooplankton. *Deep Sea Research Part A*, *36*, 1449–1456. https://doi.org/10.1016/0198-0149(89)90050-2

Chen, W., Liu, Q., Huh, C.-A., Dai, M., & Miao, Y.-C. (2010). Signature of the Mekong River plume in the western South China Sea revealed by radium isotopes. *Journal of Geophysical Research*, *115*, C12002. https://doi.org/10.1029/2010JC006460

Chen, Y. L. L., Chen, H. Y., Karl, D. M., & Takahashi, M. (2004). Nitrogen modulates phytoplankton growth in spring in the South China Sea. *Continental Shelf Research*, *24*, 527–541. https://doi.org/10.1016/j.csr.2003.12.006

Chen, Y. L. L., Chen, H. Y., Lin, Y. H., Yong, T. C., Taniuchi, Y., & Tuo, S.-H. (2014). The relative contributions of unicellular and filamentous diazotrophs to N_2 fixation in the South China Sea and the upstream Kuroshio. *Deep Sea Research, Part I*, *85*, 56–71. https://doi.org/10.1016/j.dsr.2013.11.006

Chen, Y. L. L., Chen, H. Y., Tuo, S. H., & Ohki, K. (2008). Seasonal dynamics of new production from *Trichodesmium* N_2 fixation and nitrate uptake in the upstream Kuroshio and South China Sea basin. *Limnology and Oceanography*, *53*, 1705–1721. https://doi.org/10.4319/lo.2008.53.5.1705

Deutsch, C., Gruber, N., Key, R. M., Sarmiento, J. L., & Ganachaud, A. (2001). Denitrification and N_2 fixation in the Pacific Ocean. *Global Biogeochemical Cycles*, *15*, 483–506. https://doi.org/10.1029/2000GB001291

Du, C. J., Liu, Z. Y., Kao, S. J., & Dai, M. H. (2017). Diapycnal fluxes of nutrients in an oligotrophic oceanic regime: The South China Sea. *Geophysical Research Letters*, *44*, 11,510–11,518. https://doi.org/10.1002/2017GL074921

Fawcett, S. E., Lomas, M. W., Casey, J. R., Ward, B. B., & Sigman, D. M. (2011). Assimilation of upwelled nitrate by small eukaryotes in the Sargasso Sea. *Nature Geoscience*, *4*, 717–722. https://doi.org/10.1038/ngeo1265

Fawcett, S. E., Ward, B. B., Lomas, M. W., & Sigman, D. M. (2015). Vertical decoupling of nitrate assimilation and nitrification in the Sargasso Sea. *Deep Sea Research, Part I*, *103*, 64–72. https://doi.org/10.1016/j.dsr.2015.05.004

Feuerstein, T. P., Ostrom, P. H., & Ostrom, N. E. (1997). Isotopic biogeochemistry of dissolved organic nitrogen: A new technique and application. *Organic Geochemistry*, *27*, 363–370. https://doi.org/10.1016/S0146-6380(97)00071-5

Gregg, W. W., & Casey, N. W. (2007). Sampling biases in MODIS and SeaWiFS ocean chlorophyll data. *Remote Sensing of Environment*, *111*, 25–35. https://doi.org/10.1016/j.rse.2007.03.008

Gregg, W. W., Conkright, M. E., Ginoux, P., O'Reilly, J. E., & Casey, N. W. (2003). Ocean primary production and climate: Global decadal changes. *Geophysical Research Letters*, *30*, 1809. https://doi.org/10.1029/2003GL016889

Hansell, D. A., Carlson, C. A., Repeta, D. J., & Schlitzer, R. (2009). Dissolved organic matter in the ocean: New insights stimulated by a controversy. *Oceanography*, *22*, 202–211. https://doi.org/10.5670/oceanog.2009.109

Hu, J., Kawamura, H., Hong, H., & Qi, Y. (2000). A review on the currents in the South China Sea: Seasonal circulation, South China Sea warm current and Kuroshio intrusion. *Journal of Oceanography*, *56*, 607–624. https://doi.org/10.1023/A:1011117531252

Hung, J. J., Wang, S. M., & Chen, Y. L. (2007). Biogeochemical controls on distributions and fluxes of dissolved and particulate organic carbon in the Northern South China Sea. *Deep Sea Research, Part II*, *54*, 1486–1503. https://doi.org/10.1016/j.dsr2.2007.05.006

Kao, S.-J., Terence Yang, J.-Y., Liu, K.-K., Dai, M., Chou, W.-C., Lin, H.-L., & Ren, H. (2012). Isotope constraints on particulate nitrogen source and dynamics in the upper water column of the oligotrophic South China Sea. *Global Biogeochemical Cycles*, *26*, GB2033. https://doi.org/10.1029/2011GB004091

Karl, D. M., & Church, M. J. (2017). Ecosystem structure and dynamics in the North Pacific Subtropical Gyre: New views of an old ocean. *Ecosystems*, *20*, 433–457. https://doi.org/10.1007/s10021-017-0117-0

Kessler, W. S. (2006). The circulation of the eastern tropical Pacific: A review. *Progress in Oceanography*, *69*(2–4), 181–217. https://doi.org/10.1016/j.pocean.2006.03.009

Kim, T.-W., Lee, K., Duce, R., & Liss, P. (2014). Impact of atmospheric nitrogen deposition on phytoplankton productivity in the South China Sea. *Geophysical Research Letters*, *41*, 3156–3162. https://doi.org/10.1002/2014GL059665

Knapp, A. N., Casciotti, K. L., Berelson, W. M., Prokopenko, M. G., & Capone, D. G. (2016). Low rates of nitrogen fixation in eastern tropical South Pacific surface waters. *Proceedings of the National Academy of Sciences*, *113*, 4398–4403. https://doi.org/10.1073/pnas.1515641113

Knapp, A. N., Casciotti, K. L., & Prokopenko, M. G. (2018). Dissolved organic nitrogen production and consumption in Eastern Tropical South Pacific surface waters. *Global Biogeochemical Cycles*, *32*, 769–783. https://doi.org/10.1029/2017GB005875

Knapp, A. N., DiFiore, P. J., Deutsch, C., Sigman, D. M., & Lipschultz, F. (2008). Nitrate isotopic composition between Bermuda and Puerto Rico: Implications for N_2 fixation in the Atlantic Ocean. *Global Biogeochemical Cycles*, *22*, GB3014. https://doi.org/10.1029/2007GB003107

Knapp, A. N., Sigman, D. M., Kustka, A. B., Sañudo-Wilhelmy, S. A., & Capone, D. G. (2012). The distinct nitrogen isotopic compositions of low and high molecular weight marine DON. *Marine Chemistry*, *136–137*, 24–33. https://doi.org/10.1016/j.marchem.2012.05.001

Knapp, A. N., Sigman, D. M., & Lipschultz, F. (2005). N isotopic composition of dissolved organic nitrogen and nitrate at the Bermuda Atlantic Time-series Study site. *Global Biogeochemical Cycles*, *19*, GB1018. https://doi.org/10.1029/2004GB002320

Knapp, A. N., Sigman, D. M., Lipschultz, F., Kustka, A. B., & Capone, D. G. (2011). Interbasin isotopic correspondence between upper-ocean bulk DON and subsurface nitrate and its implications for marine nitrogen cycling. *Global Biogeochemical Cycles*, *25*, GB4004. https://doi.org/10.1029/2010GB003878

Ku, H. H. (1966). Notes on the use of propagation of error formulas. *Journal of Research of the National Bureau of Standards*, *70*, 263–273. https://doi.org/10.6028/jres.070C.025

Lehmann, N., Granger, J., Kienast, M., Brown, K. S., Rafter, P. A., Martínez-Méndez, G., & Mohtadi, M. (2018). Isotopic evidence for the evolution of subsurface nitrate in the western equatorial Pacific. *Journal of Geophysical Research: Oceans*, *123*, 1684–1707. https://doi.org/10.1002/2017JC013527

Letscher, R. T., Hansell, D. A., Carlson, C. A., Lumpkin, R., & Knapp, A. N. (2013). Dissolved organic nitrogen in the global surface ocean: Distribution and fate. *Global Biogeochemical Cycles*, *27*, 141–153. https://doi.org/10.1029/2012GB004449

Letscher, R. T., Primeau, F., & Moore, J. K. (2016). Nutrient budgets in the subtropical ocean gyres dominated by lateral transport. *Nature Geoscience*, *9*, 815–819. https://doi.org/10.1038/ngeo2812

Lin, I.-I., Chen, J.-P., Wong, G. T. F., Huang, C.-W., & Lien, C.-C. (2007). Aerosol input to the South China Sea: Results from the MODerate Resolution Imaging Spectro-radiometer, the Quick Scatterometer, and the Measurements of Pollution in the Troposphere Sensor. *Deep Sea Research Part II: Topical Studies in Oceanography*, *54*(14–15), 1589–1601. https://doi.org/10.1016/j.dsr2.2007.05.013

Lin, I.-I., Wong, G. T. F., Lien, C.-C., Chien, C.-Y., Huang, C.-W., & Chen, J.-P. (2009). Aerosol impact on the South China Sea biogeochemistry: An early assessment from remote sensing. *Geophysical Research Letters*, *36*, L17605. https://doi.org/10.1029/2009GL037484

Liu, K. K., Chen, Y. J., Tseng, C. M., Lin, I. I., Liu, H. B., & Snidvongs, A. (2007). The significance of phytoplankton photo-adaptation and benthic–pelagic coupling to primary production in the South China Sea: Observations and numerical investigations. *Deep Sea Research, Part II*, *54*, 1546–1574. https://doi.org/10.1016/j.dsr2.2007.05.009

Liu, K. K., & Kaplan, I. R. (1989). The eastern tropical Pacific as a source of ^{15}N-enriched nitrate in seawater off southern California. *Limnology and Oceanography*, *34*, 820–830. https://doi.org/10.4319/lo.1989.34.5.0820

Liu, K. K., Su, M. J., Hsueh, C. R., & Gong, G. C. (1996). The nitrogen isotopic composition of nitrate in the Kuroshio Water northeast of Taiwan: Evidence for nitrogen fixation as a source of isotopically light nitrate. *Marine Chemistry*, *54*, 273–292. https://doi.org/10.1016/0304-4203(96)00034-5

Liu, K. K., Tseng, C. M., Wu, C. R., & Lin, I. I. (2010). The South China Sea. In K. K. Liu, L. Atkinson, R. Quiñones, L. Talaue-McManus (Eds.), *Carbon and nutrient fluxes in continental margins: A global synthesis* (pp. 464–482). Stockholm: Springer.

Liu, K. K., Wang, L.-W., Dai, M., Tseng, C., Yang, Y., Sui, C.-H., et al. (2013). Inter-annual variation of chlorophyll in the northern South China Sea observed at the SEATS Station and its asymmetric responses to climate oscillation. *Biogeosciences*, *10*, 7449–7462. https://doi.org/10.5194/bg-10-7449-2013

Liu, Z., & Gan, J. (2017). Three-dimensional pathways of water masses in the South China Sea: A modeling study. *Journal of Geophysical Research: Oceans*, *122*, 6039–6054. https://doi.org/10.1002/2016JC012511

Lu, Y., Wen, Z., Shi, D., Lin, W., Bonnet, S., Dai, M., & Kao, S.-J. (2019). Biogeography of N2 fixation influenced by the western boundary current intrusion in the South China Sea. *Journal of Geophysical Research: Oceans*, *124*, 6983–6996. https://doi.org/10.1029/2018jc014781

Macko, S. A., Estep, M. L. F., Engel, M. H., & Hare, P. E. (1986). Kinetic fractionation of stable nitrogen isotopes during amino acid transamination. *Geochimica et Cosmochimica Acta*, *50*, 2143–2146. https://doi.org/10.1016/0016-7037(86)90068-2

Macko, S. A., Fogel, M. L., Hare, P. E., & Hoering, T. C. (1987). Isotopic fractionation of nitrogen and carbon in the synthesis of amino acids by microorganisms. *Chemical Geology: Isotope Geoscience*, *65*, 79–92. https://doi.org/10.1016/0168-9622(87)90064-9

McRose, D. L., Lee, A., Kopf, S. H., Baars, O., Kraepiel, A. M. L., Sigman, D. M., et al. (2019). Effect of iron limitation on the isotopic composition of cellular and released fixed nitrogen in Azotobacter vinelandii. *Geochimica et Cosmochimica Acta*, *244*, 12–23. https://doi.org/10.1016/j.gca.2018.09.023

Minagawa, M., & Wada, E. (1986). Nitrogen isotope ratios of red tide organisms in the East China Sea: A characterization of biological nitrogen fixation. *Marine Chemistry*, *19*, 245–249. https://doi.org/10.1016/0304-4203(86)90026-5

Montoya, J. P., Carpenter, E. J., & Capone, D. G. (2002). Nitrogen fixation and nitrogen isotope abundances in zooplankton of the oligotrophic North Atlantic. *Limnology and Oceanography*, *47*, 1617–1628. https://doi.org/10.4319/lo.2002.47.6.1617

Moore, T. S., Campbell, J. W., & Dowell, M. D. (2009). A class-based approach to characterizing and mapping the uncertainty of the MODIS ocean chlorophyll product. *Remote Sensing of Environment*, *113*, 2424–2430. https://doi.org/10.1016/j.rse.2009.07.016

Pennington, J. T., Mahoney, K. L., Kuwahara, V. S., Kolber, D. D., Calienes, R., & Chavez, F. P. (2006). Primary production in the eastern tropical Pacific: A review. *Progress in Oceanography*, *69*, 285–317. https://doi.org/10.1016/j.pocean.2006.03.012

Peters, B. D., Lam, P. J., & Casciotti, K. L. (2018). Nitrogen and oxygen isotope measurements of nitrate along the US GEOTRACES Eastern Pacific Zonal Transect (GP16) yield insights into nitrate supply, remineralization, and water mass transport. *Marine Chemistry*, *201*, 137–150. https://doi.org/10.1016/j.marchem.2017.09.009

Ren, H., Chen, Y.-C., Wang, X. T., Wong, G. T. F., Cohen, A. L., DeCarlo, T. M., et al. (2017). 21st-century rise in anthropogenic nitrogen deposition on a remote coral reef. *Science*, *356*(6339), 749–752. https://doi.org/10.1126/science.aal3869

Ren, H., Sigman, D. M., Martínez-García, A., Anderson, R. F., Chen, M.-T., Ravelo, A. C., et al. (2017). Impact of glacial/interglacial sea level change on the ocean nitrogen cycle. *Proceedings of the National Academy of Sciences*, *114*, E6759–E6766. https://doi.org/10.1073/pnas.1701315114

Ren, H., Sigman, D. M., Meckler, A. N., Plessen, B., Robinson, R. S., Rosenthal, Y., & Haug, G. H. (2009). Foraminiferal isotope evidence of reduced nitrogen fixation in the ice age Atlantic Ocean. *Science*, *323*(5911), 244–248. https://doi.org/10.1126/science.1165787

Saba, V. S., Friedrichs, M. A. M., Carr, M.-E., Antoine, D., Armstrong, R. A., Asanuma, I., et al. (2010). Challenges of modeling depth-integrated marine primary productivity over multiple decades: A case study at BATS and HOT. *Global Biogeochemical Cycles*, *24*, GB3020. https://doi.org/10.1029/2009GB003655

Shang, S., Lee, Z., & Wei, G. (2011). Characterization of MODIS-derived euphotic zone depth: Results for the China Sea. *Remote Sensing of Environment*, *115*, 180–186. https://doi.org/10.1016/j.rse.2010.08.016

Shiozaki, T., Chen, Y.-l. L., Lin, Y.-H., Taniuchi, Y., Sheu, D.-S., Furuya, K., & Chen, H.-Y. (2014). Seasonal variations of unicellular diazotroph groups A and B, and Trichodesmium in the northern South China Sea and neighboring upstream Kuroshio Current. *Continental Shelf Research*, *80*, 20–31. https://doi.org/10.1016/j.csr.2014.02.015

Sigman, D. M., Casciotti, K. L., Andreani, M., Barford, C., Galanter, M., & Bohlke, J. K. (2001). A bacterial method for the nitrogen isotopic analysis of nitrate in seawater and freshwater. *Analytical Chemistry*, *73*(17), 4145–4153. https://doi.org/10.1021/ac010088e

Sigman, D. M., DiFiore, P. J., Hain, M. P., Deutsch, C., & Karl, D. M. (2009). Sinking organic matter spreads the nitrogen isotope signal of pelagic denitrification in the North Pacific. *Geophysical Research Letters*, *36*, L08605. https://doi.org/10.1029/2008GL035784

Sigman, D. M., & Fripiat, F. (2019). Nitrogen isotopes in the ocean. In J. K. Cochran, H. J. Bokuniewicz, P. L. Yager (Eds.), *Encyclopedia of ocean sciences* (Third ed., pp. 263–278). Oxford: Academic Press.

Silfer, J. A., Engel, M. H., & Macko, S. A. (1992). Kinetic fractionation of stable carbon and nitrogen isotopes during peptide bond hydrolysis: Experimental evidence and geochemical implications. *Chemical Geology: Isotope Geoscience*, *101*, 211–221. https://doi.org/10.1016/0009-2541(92)90003-N

Sipler, R. E., & Bronk, D. A. (2014). Dynamics of dissolved organic nitrogen. In D. A. Hansell & C. A. Carlson (Eds.), *Biogeochemistry of marine dissolved organic matter* (Second ed., pp. 127–232). Boston: Academic Press.

Torres-Valdés, S., Roussenov, V. M., Sanders, R., Reynolds, S., Pan, X., Mather, R., et al. (2009). Distribution of dissolved organic nutrients and their effect on export production over the Atlantic Ocean. *Global Biogeochemical Cycles*, *23*, GB4019. https://doi.org/10.1029/2008GB003389

Treibergs, L., Fawcett, S., Lomas, M., & Sigman, D. (2014). Nitrogen isotopic response of prokaryotic and eukaryotic phytoplankton to nitrate availability in Sargasso Sea surface waters. *Limnology and Oceanography*, *59*, 972–985. https://doi.org/10.4319/lo.2014.59.3.0972

Voss, M., Bombar, D., Loick, N., & Dippner, J. (2006). Riverine influence on N_2 fixation in the upwelling region of Vietnam, South China Sea. *Geophysical Research Letters*, *33*, L07604. https://doi.org/10.1029/2005GL025569

Wang, J.-J., & Tang, D. L. (2014). Phytoplankton patchiness during spring intermonsoon in western coast of South China Sea. *Deep Sea Research, Part II*, *101*, 120–128. https://doi.org/10.1016/j.dsr2.2013.09.020

Wang, W.-L., Moore, J. K., Martiny, A. C., & Primeau, F. W. (2019). Convergent estimates of marine nitrogen fixation. *Nature*, *566*(7743), 205–211. https://doi.org/10.1038/s41586-019-0911-2

Wang, X. T., Cohen, A. L., Luu, V., Ren, H., Su, Z., Haug, G. H., & Sigman, D. M. (2018). Natural forcing of the North Atlantic nitrogen cycle in the Anthropocene. *Proceedings of the National Academy of Sciences*, *115*, 10,606–10,611. https://doi.org/10.1073/pnas.1801049115

Wang, X. T., Sigman, D. M., Cohen, A. L., Sinclair, D. J., Sherrell, R. M., Weigand, M. A., et al. (2015). Isotopic composition of skeleton-bound organic nitrogen in reef-building symbiotic corals: A new method and proxy evaluation at Bermuda. *Geochimica et Cosmochimica Acta*, *148*, 179–190. https://doi.org/10.1016/j.gca.2014.09.017

Waser, N. A. D., Harrison, W. G., Head, E. J. H., Nielsen, B., Lutz, V. A., & Calvert, E. S. (2000). Geographic variations in the nitrogen isotope composition of surface particulate nitrogen and new production across the North Atlantic Ocean. *Deep Sea Research, Part I*, *47*, 1207–1226. https://doi.org/10.1016/S0967-0637(99)00102-8

Weigand, M. A., Foriel, J., Barnett, B., Oleynik, S., & Sigman, D. M. (2016). Updates to instrumentation and protocols for isotopic analysis of nitrate by the denitrifier method. *Rapid Communications in Mass Spectrometry*, *30*(12), 1365–1383. https://doi.org/10.1002/rcm.7570

Wong, G. T. F., Tseng, C. M., Wen, L. S., & Chung, S. W. (2007). Nutrient dynamics and N-anomaly at the SEATS station. *Deep Sea Research, Part II*, *54*, 1528–1545. https://doi.org/10.1016/j.dsr2.2007.05.011

Wu, J., Chung, S. W., Wen, L. S., Liu, K. K., Chen, Y. L. L., Chen, H. Y., & Karl, D. M. (2003). Dissolved inorganic phosphorus, dissolved iron, and *Trichodesmium* in the oligotrophic South China Sea. *Global Biogeochem Cycles*, *17*, 1008. https://doi.org/10.1029/2002GB001924

Xiao, H. W., Xiao, H. Y., Luo, L., Zhang, Z. Y., Huang, Q. W., Sun, Q. B., & Zeng, Z. Q. (2018). Stable carbon and nitrogen isotope compositions of bulk aerosol samples over the South China Sea. *Atmospheric Environment*, *193*, 1–10. https://doi.org/10.1016/j.atmosenv.2018.09.006

Xu, M. N., Zhang, W., Zhu, Y., Liu, L., Zheng, Z., Wan, X. S., et al. (2018). Enhanced ammonia oxidation caused by lateral Kuroshio intrusion in the boundary zone of the northern South China Sea. *Geophysical Research Letters*, *45*, 6585–6593. https://doi.org/10.1029/2018GL077896

Yamaguchi, Y. T., & McCarthy, M. D. (2018). Sources and transformation of dissolved and particulate organic nitrogen in the North Pacific Subtropical Gyre indicated by compound-specific $\delta^{15}N$ analysis of amino acids. *Geochimica et Cosmochimica Acta*, *220*, 329–347. https://doi.org/10.1016/j.gca.2017.07.036

Yang, J.-Y. T., Hsu, S.-C., Dai, M., Hsiao, S. S.-Y., & Kao, S.-J. (2014). Isotopic composition of water-soluble nitrate in bulk atmospheric deposition at Dongsha Island: Sources and implications of external N supply to the northern South China Sea. *Biogeosciences*, *11*, 1833–1846. https://doi.org/10.5194/bg-11-1833-2014

Yang, J.-Y. T., Kao, S.-J., Dai, M., Yan, X., & Lin, H.-L. (2017). Examining N cycling in the northern South China Sea from N isotopic signals in nitrate and particulate phases. *Journal of Geophysical Research: Biogeosciences*, *122*, 2118–2136. https://doi.org/10.1002/2016JG003618

Yang, Z., Chen, J., Chen, M., Ran, L., Li, H., Lin, P., et al. (2018). Sources and transformations of nitrogen in the South China Sea: Insights from nitrogen isotopes. *Journal of Oceanography*, *74*, 101–113. https://doi.org/10.1007/s10872-017-0443-z

Zerkle, A. L., Junium, C. K., Canfield, D. E., & House, C. H. (2008). Production of ^{15}N-depleted biomass during cyanobacterial N_2-fixation at high Fe concentrations. *Journal of Geophysical Research*, *113*, G03014. https://doi.org/10.1029/2007JG000651

Zhang, R., Chen, M., Ma, Q., Cao, J., & Qiu, Y. (2011). Latitudinal distribution of nitrogen isotopic composition in suspended particulate organic matter in tropical/subtropical seas. *Isotopes in Environmental and Health Studies*, *47*(4), 489–497. https://doi.org/10.1080/10256016.2011.622442

Zhang, R., Chen, M., Yang, Q., Lin, Y., Mao, H., Qiu, Y., et al. (2015). Physical-biological coupling of N_2 fixation in the northwestern South China Sea coastal upwelling during summer. *Limnology and Oceanography*, *60*, 1411–1425. https://doi.org/10.1002/lno.10111

Zhang, C., Hu, C., Shang, S., Müller-Karger, F. E., Li, Y., Dai, M., et al. (2006). Bridging between SeaWiFS and MODIS for continuity of chlorophyll-*a* concentration assessments off Southeastern China. *Remote Sensing of Environment*, *102*, 250–263. https://doi.org/10.1016/j.rse.2006.02.015